

UNIVERSITY OF SOUTHERN CALIFORNIA
DEPARTMENT OF CIVIL ENGINEERING

CORRELATIONS OF THE FREQUENCY DEPENDENT DURATION
OF STRONG EARTHQUAKE GROUND MOTION WITH THE MAGNITUDE,
EPICENTRAL DISTANCE, AND THE DEPTH OF SEDIMENTS AT THE
RECORDING SITE

by

B.D. Westermo and M.D. Trifunac

Report No. CE 78-12

A Report on Research Conducted Under a Contract
from the Nuclear Regulatory Commission

Los Angeles, California

September, 1978

ABSTRACT

In this report, we present empirical models for estimation of the duration of strong earthquake ground shaking and two related functionals in terms of earthquake magnitude, epicentral distance, horizontal or vertical direction of motion and the depth of sediments beneath the recording station. These models represent a refinement of the similar regression analysis (Trifunac and Westermo, 1976a) in terms of rough site classification $s=0, 1$ and 2 corresponding to alluvium, intermediate and hard rock sites.

INTRODUCTION

Correlations of some of the characteristics of strong ground motion, e.g., the duration, or $\int_0^t \{a^2(\tau), v^2(\tau), d^2(\tau)\} d\tau$, with the recording site classification have shown that these quantities are significantly dependent on the site characteristics. The effect of the geological conditions at the recording site on the strong ground motion has been previously examined through these correlations by classifying the site into either $s=0$, 1 or 2, where $s=0$ represents alluvium or sediments, $s=2$ represents hard rock, and $s=1$ represents intermediate sites. Although this form of site characterization showed the general dependence of ground motion on the geologic site characteristics, it represents only a crude and approximate classification satisfactory for site effect analysis when no other information on the local geology is available.

A more detailed description of the site geology for correlations with the characteristics of the recorded strong ground motion could be given by the depth of the alluvial or sedimentary layer(s) at the site on top of the harder, basement rock. It is this dimension, together with the impedance variations, that should govern the general nature of the wave propagation characteristics in the vicinity of the recording site (Wong and Trifunac, 1977).

In this report, we examine the correlations of a) the duration of strong shaking, b) the integrals of acceleration, velocity, and displacement squared, and c) the average time rate of growth of these

integrals in six narrow frequency bands with the earthquake magnitude, the epicentral distance, and the depth of the sedimentary layer at the recording site. The distributions of the data about the developed models are also presented.

DEFINITIONS

The definition of the duration of strong ground motion used in this report is based on the growth in time of the integrals

$$\int_0^t \left\{ \begin{array}{l} a^2(\tau) \\ v^2(\tau) \\ d^2(\tau) \end{array} \right\} dt .$$

Functionals of this type have been widely used in earthquake engineering as they are found in the definitions of the instrumental intensity, the seismic wave energy, and the power spectrum width (Trifunac and Westermo, 1976a). The general behavior of these integrals is to increase rapidly with the large amplitudes of incoming waves and to gradually trail off to their final values,

$$\int_0^T \left\{ \begin{array}{l} a^2 \\ v^2 \\ d^2 \end{array} \right\} dt ,$$

where T is the total duration of the record, with the arrivals of the scattered waves attenuated by their longer propagation paths. As in our previous studies (Trifunac and Westermo, 1976a,b), we define the duration of strong ground motion at a particular frequency band to be the sum of the time intervals over which the largest contribution to the integral of the band filtered acceleration, velocity, or displacement squared is made. This definition was also chosen such that the duration is explicitly independent of the amplitudes of

$$\int_0^T \left\{ \begin{array}{l} a^2 \\ v^2 \\ d^2 \end{array} \right\} dt .$$

Figure 1 summarizes the procedure of Trifunac and Westermo (1976a)

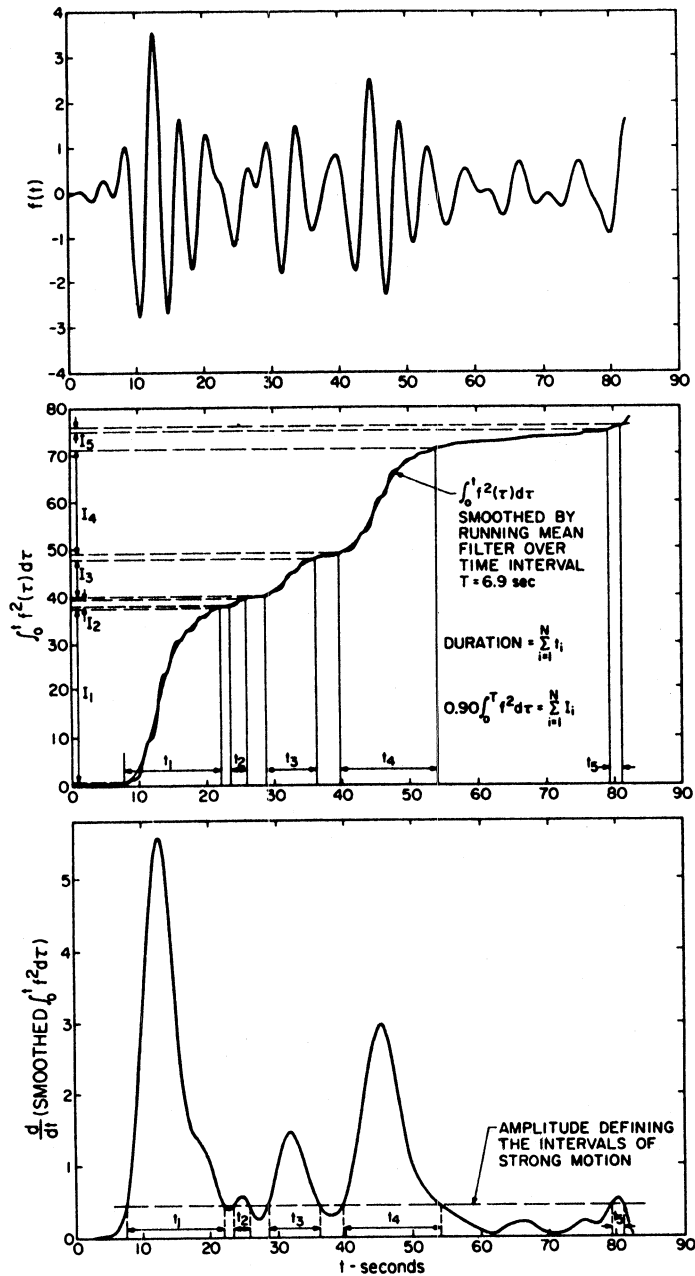


FIGURE 1

(Top) Displacement record for Kern County earthquake after applying bandpass filter centered at 0.22 Hz

(Center) Comparison of $\int_0^t f^2(\tau) d\tau$ computed for $f(t)$ (above) with its smoothed form

(Bottom) The derivative of the smoothed function, $\frac{d}{dt} \int_0^t f^2(\tau) d\tau$, showing the time intervals of strong motion as defined in this study

used in defining and calculating the duration of a frequency-filtered record. The time intervals of the largest contribution to $\int_0^t f^2(\tau)d\tau$, where $f(t)$ represents either the acceleration, velocity, or displacement, are the intervals over which the slopes of the integral are greater than some specified level (dashed line at the bottom of Figure 1). This level is chosen such that the contributions to $\int_0^t f^2(\tau)d\tau$ during the chosen time intervals make up 90% of the final value of $\int_0^t f^2 d\tau$. The $\int_0^t f^2 d\tau$ curve is first smoothed with a running mean filter before differentiating to avoid having too many contributing intervals (particularly for the high frequency records) and yet without significantly altering the calculated duration. Table I lists the filter windows used in this procedure for each frequency band of data.

Employing this definition of duration we define the average rate of growth of the integrals of strong shaking as

$$\text{RATE} \begin{Bmatrix} a(t) \\ v(t) \\ d(t) \end{Bmatrix} = \int_0^T \begin{Bmatrix} a^2(\tau) \\ v^2(\tau) \\ d^2(\tau) \end{Bmatrix} d\tau / \text{DURATION} \begin{Bmatrix} a \\ v \\ d \end{Bmatrix} . \quad (1)$$

This "rate" is essentially the slope of $\int_0^t f^2 d\tau$ averaged over the sum of the intervals of strong motion and thus is a measure of the time rate at which the quantities $\int_0^t \{a^2, v^2, d^2\} d\tau$ increase. The rate is indicative of whether the major portions of the input "energy," $\int_0^t \{a^2, v^2, d^2\} d\tau$, are fed into the receiver over a long or short time period, thus determining the potential damage to a structure that can accommodate only a fixed amount of input energy, or strong shaking amplitude, per unit of time.

TABLE I

Roll-Off and Termination Frequencies for the Six Low-Pass Ormsby Filters and Filter Windows for Smoothing the Integrals

$$\int_0^t f^2(\tau) d\tau$$

| <u>Band No.</u> | <u>Low-Pass Roll-Off Frequency (cps)</u> | <u>Low-Pass Termination Frequency (cps)</u> | <u>Center Frequency (cps)</u> | <u>Filter Window* (sec)</u> |
|-----------------|--|---|-------------------------------|-----------------------------|
| 1 | 9.1 | 10.9 | 18.0 | 3.38 |
| 2 | 3.6 | 4.4 | 7.0 | 3.38 |
| 3 | 1.34 | 1.66 | 2.7 | 3.38 |
| 4 | 0.62 | 0.78 | 1.1 | 4.08 |
| 5 | 0.26 | 0.34 | 0.5 | 4.08 |
| 6 | 0.105 | 0.125 | 0.2 | 6.9 |

* Filter window represents the time interval in seconds over which the running mean filter was used to low-pass filter $\int_0^t f^2(\tau) d\tau$ (see also Figure 1).

A more detailed discussion of the three quantities $\int_0^t f^2 d\tau$, duration, and the rate is given in our previous reports (Trifunac and Westermo, 1976a,b).

DESCRIPTION OF THE DATA

The acceleration, velocity and displacement data used in this study are from the Volume II tapes (Trifunac and Lee, 1973) which contain the corrected accelerograms and the integrated velocity and displacement curves. These data consist of 186 complete records (372 horizontal component records and 186 vertical component records) which were obtained at free-field stations or in the basement floors of buildings. These data were the result of 49 earthquakes whose magnitudes range from 3.0 to 7.7. Of the 186 records, 5 or 3% correspond to the magnitude range 4.0 to 4.9, 40 or 22% to 5.0 to 5.9, 126 or 69% to 6.0 to 6.9, and 7 or 4% to the range 7.0 to 7.9. Six of the 186 records were not used in the correlations with magnitude due to incomplete information on the magnitude.

The complete records from Volume II tapes were filtered with an Ormsby digital low-pass filter in succession by filtering each low-pass filtered record with a progressively lower roll-off and termination frequency. The sum of the six frequency band filtered records adds up to the original record. Table I lists the termination and roll-off frequency^{*} used for each frequency band. The entire data package used in this study is identical to that used in our previous studies (Trifunac and Westermo, 1976a,b).

The depth of sedimentary deposits was computed from differences in elevation between the ground surface and the contact of alluvium

* In the rest of this report each frequency band will be referred to by its center frequency, $f_c = 18.0, 7.0, 2.75, 1.1, 0.5, \text{ and } 0.22 \text{ Hz.}$

and sedimentary layers with crystalline basement rocks. The principle which governed our judgement in assigning the "depth" to each of the station sites, where the 186 strong motions have been recorded, was that this characteristic dimension should have the strongest influence on the recording site effects (Wong and Trifunac, 1977). It is clear, of course, that a single dimension is far from sufficient to characterize all three-dimensional details of geologic strata beneath each station. Needless to say, classifying the site effects by this depth states nothing about the impedance changes of earth materials within the chosen range of depth. Remembering, however, that (1) for many strong motion sites shear wave velocity increases from about 1 km/sec near surface to ~ 3 km/sec near interface between sediments and the basement rock where it jumps to higher values and (2) that the horizontal characteristic length of sedimentary deposits is often considerably longer than its vertical thickness, we choose to explore the possibility of refining our previous site classification in terms of $s=0, 1$ and 2 , by replacing s with the "depth" of sediments, h , at each recording station. Although considerable judgement and oversimplification were required before each station could be assigned a depth parameter, it appeared useful to explore to what extent the trends in recorded data could be related to an estimate of a depth parameter, before more refined site characterization is attempted and justified. The results of this and of several related investigations showed that the above definition of depth is useful and better than our previous characterizations in terms of $s=0, 1$ or 2 . In future

reports, a detailed account will be presented on all available information and on all procedures used in arriving at an estimate of the depth of sediments at strong motion stations where the 186 records have been recorded.

Figure 2 presents a histogram of all depths used in this study. It shows a fairly uniform coverage for depths between 0 and 4 km. The sites classified as $s=2$ (basement rock) in our previous work (Trifunac and Westermo, 1976a) are now assigned $h=0$ km.

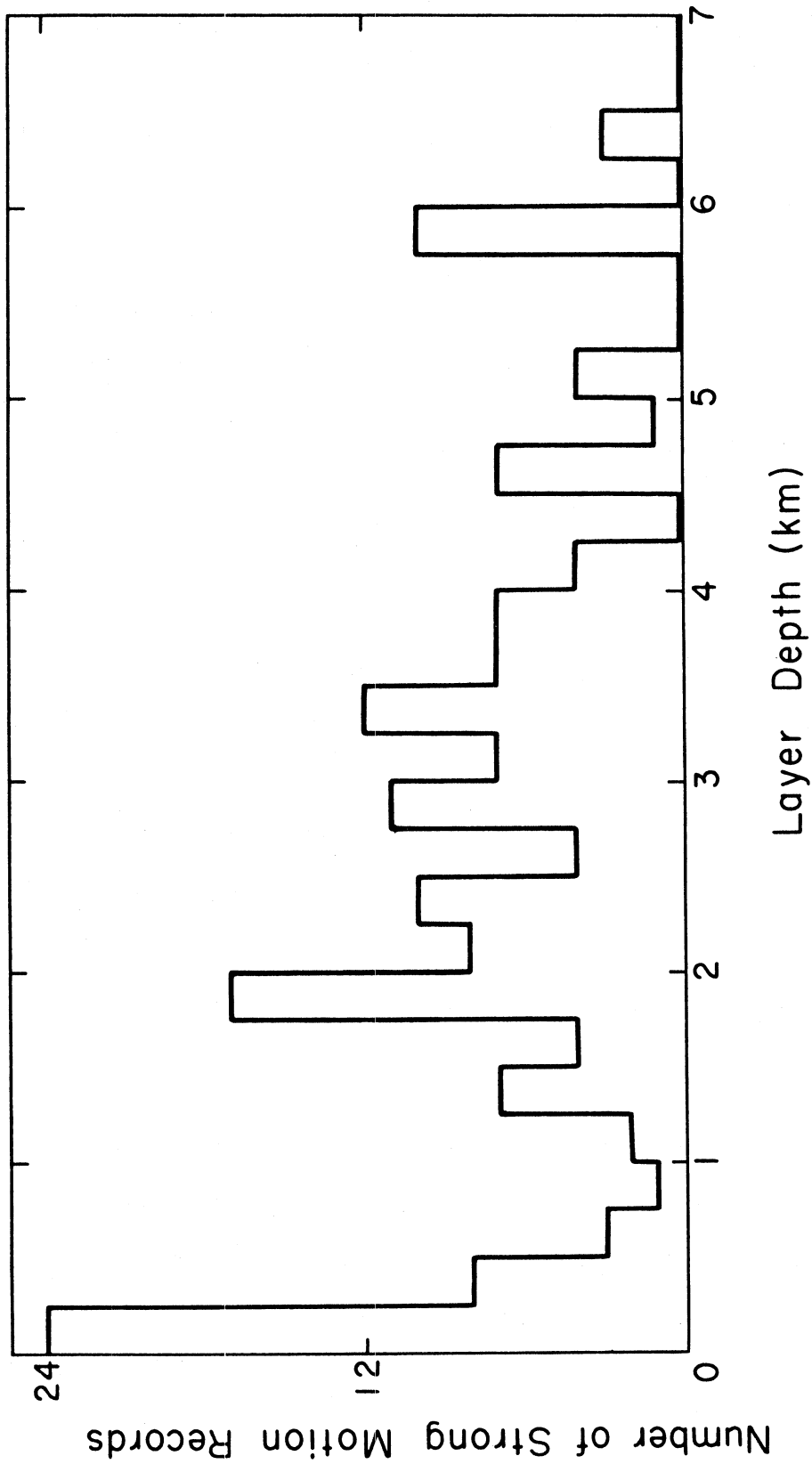


FIGURE 2
Histogram of the distribution of the depths at the recording sites for the 186 records used in this study

REGRESSION MODELS OF THE FREQUENCY DEPENDENT DURATION OF
STRONG GROUND MOTION IN TERMS OF THE MAGNITUDE, EPICENTRAL DISTANCE
AND DEPTH OF SEDIMENTS

To develop an empirical model which describes the dependence of the duration on the parameters characterizing the earthquake and the recording site geology, the duration is interpreted as being a function of the motion at the earthquake source, the characteristics of the medium through which the waves travel, and the characteristics of the geology in the vicinity of the receiver. We assume that the duration for a narrow frequency band of motion is the sum of these three contributions (Trifunac and Brady, 1975), where

$$\text{Duration of strong motion} \approx d_{\text{source}} + d_{\Delta} + d_{\text{site}} . \quad (2)$$

The term d_{source} in the above equation represents the duration of the shaking at the source. For an approximate characterization of d_{source} , it is assumed that the source motion is a result of a dislocation propagating with speed v along a straight fault of length L . The duration of strong motion at the fault, d_{source} , then, is approximately the total time length of faulting plus the directional effect of the dislocation propagation. Thus,

$$d_{\text{source}} \approx L \left(\frac{1}{v} - \frac{\cos\alpha}{\beta} \right) , \quad (3)$$

where β is the wave speed near the fault and α is the azimuthal angle between the vectors describing the dislocation propagation and the position of the receiver from the source. In this study, as in our previous reports (Trifunac and Brady, 1975; Trifunac and Westermo, 1976a), we have used only the magnitude to describe the earthquake

source as it is often a characteristic of the strong motion available for many earthquakes. Although equation (3) and other idealized source models may suggest the use of parameters such as L , v and α for an approximation of the duration, these quantities are not so readily or accurately obtainable, and their use in correlations with the duration would limit the range of applications of the empirical model. Since the functional dependence of the duration through L on the magnitude is not yet well known (Trifunac and Westermo, 1976a), we propose to define the source contribution to the duration in the simple, linear form

$$d_{\text{source}} = b(\omega_c)M \quad . \quad (4)$$

The coefficient $b(\omega_c)$ is a function of the center frequency of each band and of the direction of motion.

A quadratic function of the form

$$d_{\text{source}} = b(\omega_c)M + c(\omega_c)M^2$$

was also fit to the data. The resulting coefficient $c(\omega_c)$ was not significantly different from zero at the 95% confidence level. This is probably due to the limited range of magnitude data (90% of all available data is for $5 \leq M \leq 7$).

The contribution to the duration resulting from the dispersion of the seismic waves, d_{Δ} , is assumed to be the time difference between the arrival of the fastest and the slowest traveling waves. This assumption, also applied in our previous studies (Trifunac and Brady, 1975; Trifunac and Westermo, 1976a), implies a dependence of d_{Δ} on the epicentral distance of the form

$$d_{\Delta} = c(\omega_c)\Delta \quad (5)$$

where $c(\omega_c)$ is interpreted as

$$c = \frac{1}{v_{\min}} - \frac{1}{v_{\max}} .$$

v_{\min} and v_{\max} are the minimum and maximum wave speeds, respectively, for the frequency band considered. Since the dispersive characteristics of the local geology would depend upon the overall layer thickness, we attempted to determine the dependence of the dispersion coefficient in equation (5), $c(\omega_c)$, on the depth, h . It was assumed that $c(\omega_c)$ was a quadratic function of the depth and the dispersion related contribution to the duration was taken as,

$$d_{\Delta} = \{c_1(\omega_c) + c_2(\omega_c)h + c_3(\omega_c)h^2\}\Delta . \quad (6)$$

The values of the coefficients c_2 and c_3 resulting from the regression of equation (6) with the data were not significantly different from zero at a 95% confidence level and thus were not used in the final duration model. It is concluded that the dispersion coefficient, $c(\omega_c)$, may not correlate well with the depth of sediments or that the variations in the local geology that affect the dispersion are not very sensitive to the variations of layer thickness. The value of the coefficient $c(\omega_c)$ in equation (5) was found to be significant at the 95% confidence level and equation (5) was chosen to approximate the dispersion dependent part of the duration.

The functional dependence of the contribution to the duration from the site geology, d_{site} , on the depth of sediments is not well understood to imply a particular functional form. To determine the

simplified dependence of d_{site} on depth, the recording site is modeled as a layer over a homogeneous half space. For depths much smaller than the wavelengths considered, the effect of this layer on duration should be negligible and hence d_{site} is expected to be zero for sufficiently small h . For deep layers, the ray paths of the waves in the layer reflected off the bottom will be long so that the anelastic attenuation will reduce the amplitudes of these reflections below the recording noise level. Thus, for both very large and very small depths, h (relative to the wavelength), it is expected that d_{site} should approach zero. For the intermediate depths, d_{site} is positive since the later arriving waves reflected off the layer bottom contribute to an extension of the duration. To examine this assumed trend for d_{site} we consider the relation

$$d_{\text{site}} = d_1(\omega_c)h + d_2(\omega_c)h^2 \quad (7)$$

where d_1 and d_2 are the regression coefficients. The values obtained for the coefficient d_2 were not significantly different from zero at the 95% confidence level for all frequency bands. Yet, a trend was apparent for d_{site} to increase with h between 0 km and 6 km. The inability of equation (7) to detect a significant extremum of d_{site} with respect to h could be due to the limited range of depths available (see Figure 2) in that the data does not include records at sites with large enough depths for which d_{site} ceases to grow with depth and begins to decrease due to the attenuation. It seems that the range of depths for the available data restricts the behavior of d_{site} only to growth. Hence, a simple, linear dependence of d_{site} on the depth

was chosen where

$$d_{\text{site}} = d(\omega_c) \quad . \quad (8)$$

Applying equations (4), (5) and (8) to equation (2) leads to the empirical model

$$\text{Duration} \begin{Bmatrix} a \\ v \\ d \end{Bmatrix} = a(\omega_c) + b(\omega_c)M + c(\omega_c)\Delta + d(\omega_c)h \quad , \quad (9)$$

where the coefficients a , b , c and d are functions of the acceleration, velocity and displacement; the horizontal or vertical component of motion; and the center frequency of each of the six frequency bands. The values of these coefficients were found by the least squares fitting of equation (9) to the data. If it is assumed that the band filtered records may be characterized only by the center frequency of each band, it is seen (Trifunac and Westermo, 1976a) that for a given component of motion in a particular frequency band,

$$\text{Duration}\{a(t)\} \doteq \text{Duration}\{v(t)\} \doteq \text{Duration}\{d(t)\} \quad . \quad (10)$$

The coefficients a through d for the durations of acceleration, velocity and displacement were thus combined as suggested by equation (10). The resulting coefficients a through d then represent an average of the coefficients for duration of acceleration, velocity and displacement. The vertical and horizontal components of motion were analyzed separately. As noted in the previous studies using these six band-filtered records (Trifunac and Westermo, 1976a), the signal-to-noise ratio of the displacement data for the high frequency band $f_c = 18.0$ Hz and the acceleration data for low frequency band $f_c = 0.22$ Hz was much lower than for

the rest of the frequency bands. For this reason, these two data sets were excluded from all of the correlations presented here.

To examine the distribution of the data about the model, equation (9), the residual of each data point was calculated. The residual of a data point, ϵ_i , is the difference between the actual value of duration and the value predicted by equation (9) and is equal to

$$\epsilon_i = \text{duration}_i - \{a(\omega_c) + b(\omega_c)M + c(\omega_c)\Delta + d(\omega_c)h\}, \quad i=1, N_{\text{data}} \quad (11)$$

Assuming that equation (9) is of the appropriate form for approximating the duration, the residuals can be assumed to be independent of Δ , M , or h . The parameter $p = p(\epsilon_i)$ defined here as the "confidence level," represents the fraction of data with residual values less than or equal to ϵ_i . Although this distribution $p(\epsilon_i)$ is a set of discrete points, the number of data is large enough to consider $p(\epsilon_i)$ as estimates of a continuous distribution curve $p(\epsilon)$. These empirical $p(\epsilon)$ functions were calculated for all six frequency bands and both components of motion and are shown in Figure 4. The general shape of each of these 12 curves is similar while only the numerical values of $p(\epsilon)$ vary with frequency or component of motion. To examine the type of these $p(\epsilon)$ functions, exponential distributions were fit to the $p(\epsilon_i)$ data. The respective fits were tested with both the Chi-Squared and Kolmogorov-Smirnov tests. Only the double exponential distribution passed both tests at the 95% confidence level for a majority of the frequency bands. The double exponential distribution is of the form

$$p(\epsilon) = 1 + \alpha_1 e^{\beta_1 \epsilon} + \alpha_2 e^{\beta_2 \epsilon}, \quad (12)$$

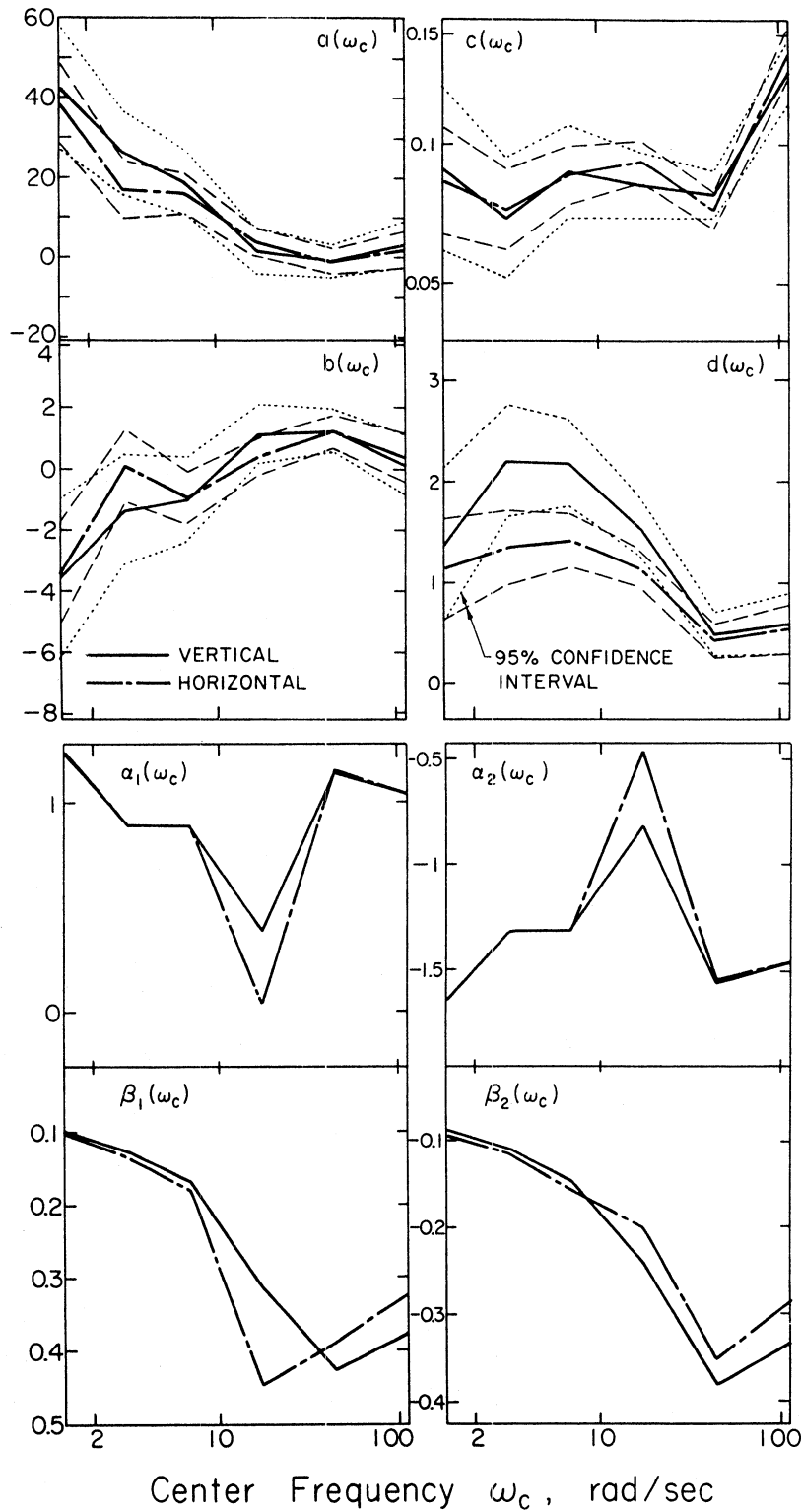


FIGURE 3

The coefficients a , b , c , d , α_1 , α_2 , β_1 , and β_2 in equations (9) and (12) for horizontal and vertical components of ground motion plotted versus $\omega_c = 2\pi f_c$ (for $f_c = 0.22, 0.5, 1.1, 2.75, 7.0,$ and 18.0 Hz). The coefficients a , b , c , and d are bounded by their estimated 95% confidence intervals.

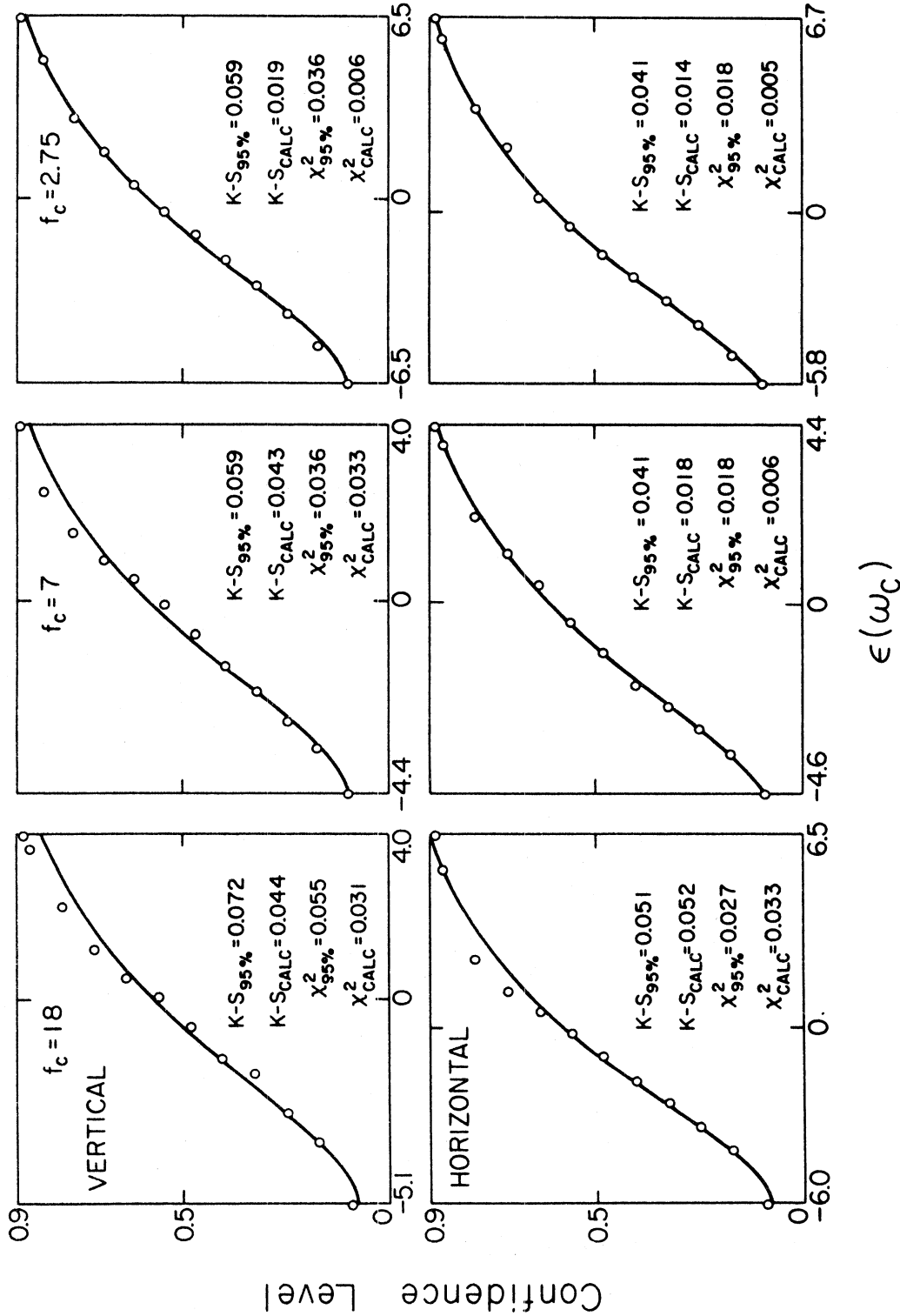
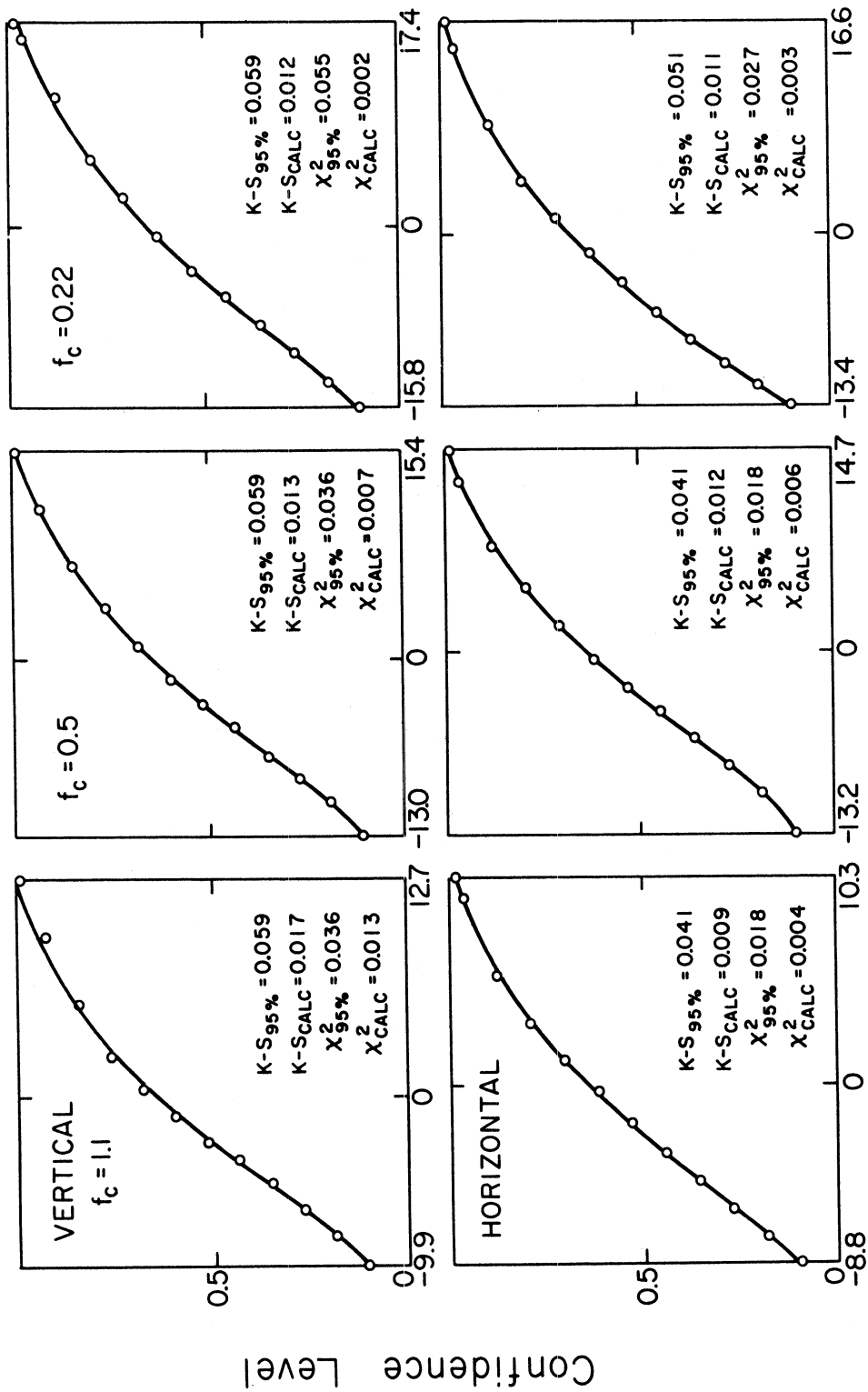


FIGURE 4a

The confidence level, p , versus the residual, ϵ , for the calculated residuals (circles) and for the fitted double exponential distribution (solid curve). The Chi-Squared and Kolmogorov-Smirnov criteria are listed for each distribution.



$\epsilon(\omega_c)$

FIGURE 4b

The confidence level, p , versus the residual, ϵ , for the calculated residuals (circles) and for the fitted double exponential distribution (solid curve). The Chi-Squared and Kolmogorov-Smirnov test criteria are listed for each distribution.

where α_1 , α_2 , β_1 , and β_2 are the four scaling parameters.

This type of distribution is common to the first passage problems where one seeks to determine the time at which a function first exceeds some given value. The definition of duration used here is similar to this class of problems in that the duration is related to the time at which the functions $\int_0^t \{a^2, v^2, d^2\} d\tau$ exceed 90% of $\int_0^T \{a^2, v^2, d^2\} d\tau$ (see Figure 1). The parameters α_1 , α_2 , β_1 and β_2 were assumed to be functions of frequency and the component of motion and were calculated by the nonlinear least squares regression of equation (12) for the $p(\epsilon)$ data. To eliminate the segments of the $p(\epsilon)$ curves which are significantly affected by the data with low signal to noise ratios or by an insufficient number of data points, the intervals $p > 0.9$ and $p < 0.1$ were ignored. Thus, the coefficients $\alpha_1(\omega_c)$, $\alpha_2(\omega_c)$, $\beta_1(\omega_c)$ and $\beta_2(\omega_c)$ represent the best fit for all of the $p(\epsilon)$ data within $0.1 \leq p \leq 0.9$. The resulting double exponential distributions are shown with some points of the $p(\epsilon_i)$ data in Figures 4a and 4b.

Table II presents the results of the regressions outlined above. The coefficients a , b , c , d , α_1 , α_2 , β_1 , and β_2 are functions of the vertical or horizontal component of motion and the center frequency of each of the six frequency bands. To describe the uncertainties associated with equation (9) the variance of each of the coefficients a , b , c and d was calculated by the procedure outlined in Appendix I. These variances are listed in Table II. The dependence of the coefficients a , b , c , and d on center frequency is shown in Figure 3. Each of the coefficient curves in this figure is surrounded by an interval

TABLE II

Regression Coefficients for

$$\text{Duration} \begin{Bmatrix} a \\ v \\ d \end{Bmatrix} = a + bM + c\Delta + dh$$

VERTICAL COMPONENT

| | $f_c = 18.$ | $f_c = 7.$ | $f_c = 2.75$ | $f_c = 1.1$ | $f_c = 0.5$ | $f_c = 0.22$ |
|--------------------|-------------|------------|--------------|-------------|-------------|--------------|
| a | 0.320 | -0.108 | 0.120 | 1.847 | 2.580 | 4.263 |
| Variance(a) (x0.1) | 0.291 | 0.208 | 0.287 | 0.411 | 0.535 | 0.792 |
| b | 0.070 | 1.216 | 1.099 | -1.022 | -1.351 | -3.598 |
| Variance(b) | 0.493 | 0.353 | 0.486 | 0.697 | 0.907 | 1.329 |
| c | 12.621 | 8.176 | 8.516 | 9.009 | 7.324 | 9.096 |
| Variance(c) (x100) | 0.598 | 0.428 | 0.590 | 0.846 | 1.101 | 1.512 |
| d | 0.592 | 0.485 | 1.525 | 2.175 | 2.198 | 1.363 |
| Variance(d) | 0.152 | 0.109 | 0.150 | 0.215 | 0.280 | 0.390 |
| α_1 | 1.034 | 1.139 | 0.396 | 0.887 | 0.890 | 1.241 |
| β_1 (x10) | -3.753 | -4.254 | -3.137 | -1.678 | -1.294 | -0.981 |
| α_2 | -1.469 | -1.563 | -0.821 | -1.311 | -1.315 | -1.660 |
| β_2 (x10) | -3.308 | -3.797 | -2.415 | -1.463 | -1.111 | -0.889 |
| No. of Data | 360 | 540 | 540 | 540 | 540 | 360 |

TABLE II
(Continued)

HORIZONTAL COMPONENT

| | $f_c = 18$ | $f_c = 7$ | $f_c = 2.75$ | $f_c = 1.1$ | $f_c = 0.5$ | $f_c = 0.22$ |
|--------------------|------------|-----------|--------------|-------------|-------------|--------------|
| a | 0.182 | -0.124 | 0.336 | 1.574 | 1.678 | 3.866 |
| Variance(a) (x0.1) | 0.236 | 0.161 | 0.182 | 0.255 | 0.357 | 0.518 |
| b | 0.317 | 1.174 | 0.398 | -0.980 | 0.057 | -3.460 |
| Variance(b) | 0.400 | 0.273 | 0.308 | 0.433 | 0.605 | 0.869 |
| c | 13.311 | 7.612 | 9.375 | 8.873 | 7.625 | 8.655 |
| Variance(c) (x100) | 0.486 | 0.335 | 0.378 | 0.530 | 0.742 | 0.990 |
| d | 0.536 | 0.412 | 1.120 | 1.411 | 1.342 | 1.129 |
| Variance(d) | 0.124 | 0.085 | 0.096 | 0.135 | 0.189 | 0.255 |
| α_1 | 1.037 | 1.152 | 0.043 | 0.891 | 0.889 | 1.250 |
| β_1 (x10) | -3.221 | -3.893 | -4.474 | -1.816 | -1.361 | -1.039 |
| α_2 | -1.464 | -1.550 | -0.460 | -1.315 | -1.320 | -1.651 |
| β_2 (x10) | -2.849 | -3.518 | -2.019 | -1.586 | -1.181 | -0.956 |
| No. of Data | 720 | 1080 | 1080 | 1080 | 1080 | 720 |

calculated from the variances (see Appendix I) and based on a 95% confidence level.

The curves of $b(\omega_c)$ in Figure 3 show the duration to decrease with increasing magnitude for the lower frequency bands ($f_c = 0.22, 0.5,$ and 1.1 Hz) and to increase with magnitude for the higher frequency bands ($f_c = 2.75, 7.0,$ and 18.0 Hz). It is also apparent from Figure 3 that $b(\omega_c) = 0$ lies within the 95% confidence intervals for $f_c = 0.22, 0.5, 1.1, 2.75,$ and 18.0 Hz. This means that the dependence of duration on magnitude may become insignificant for these frequencies. A similar trend was noticed in the correlations of duration with magnitude, epicentral distance, and $s=0, 1$ or 2 site classifications (Trifunac and Westermo, 1976a) and was postulated to result primarily from the low signal to noise ratio for small magnitude earthquakes. Since the duration is defined in this work to be independent of the overall amplitudes of strong shaking, a small magnitude earthquake would produce low amplitude waves that have a lower signal to noise ratio than large magnitude events for equivalent epicentral distances. Thus, the data on durations for low magnitude earthquakes appear to be affected by the recording, digitization, and processing noise.

The coefficient $c(\omega_c)$, as shown in Figure 3, is roughly equal to a constant ($0.8 < c < 0.9$) for the five lowest frequency bands and increases to $c \approx 0.14$ at $f_c = 18.0$ Hz. This increased dispersion at high frequencies could be due to the scattering and diffraction of the high frequency waves by the numerous inhomogeneities of small enough characteristic dimensions that they do not significantly affect the low frequency wave propagation. A similar behavior of $c(\omega_c)$ was noted in the previous

correlations by Trifunac and Westermo (1976a).

From the values of $d(\omega_c)$ shown in Figure 3, it is seen that the increase in duration with h is larger for the vertical than for horizontal motion in all of the frequency bands. For $f_c = 0.5$ and 1.1 Hz, the duration increases by roughly 2.2 secs/km for the vertical motion and by about 1.4 secs/km for the horizontal motion. For the high frequency bands $f_c = 18.0$ Hz and $f_c = 7.0$ Hz, the duration increases by about 0.6 secs/km. In comparing the correlations presented here, which depend on the depth of sediments beneath a station, with previous correlations (Figure 8 in Trifunac and Westermo, 1976a) in terms of the site classification, s , it is seen that the previous coefficient is quite similar to $d(\omega_c)$ in this study. Both correlations show a small dependence on the site conditions at the high frequencies ($f_c = 18.0$ and 7.0 Hz) and a larger dependence at $f_c = 0.22$, 0.5 , and 1.1 Hz with the vertical component being more influenced by the site condition.

The duration of strong motion as computed from equation (9) is shown in Figures 5a and 5b for selected values of magnitude, epicentral distance, and depths of sediments versus the center frequency of each band. The coefficients in equation (9) were smoothed along the frequency axis by a $(\frac{1}{4}, \frac{1}{2}, \frac{1}{4})$ filter to show the average trends of the empirical model. These plots show that the difference between the duration at low frequencies ($f_c = 0.22$ Hz) and the high frequencies ($f_c = 18.0$ Hz) can be at most about 20 seconds for the depth of sediments equal to 6 km and for zero epicentral distance. The variation of the duration with frequency tends to diminish for large magnitudes, large epicentral distance, and small depths.

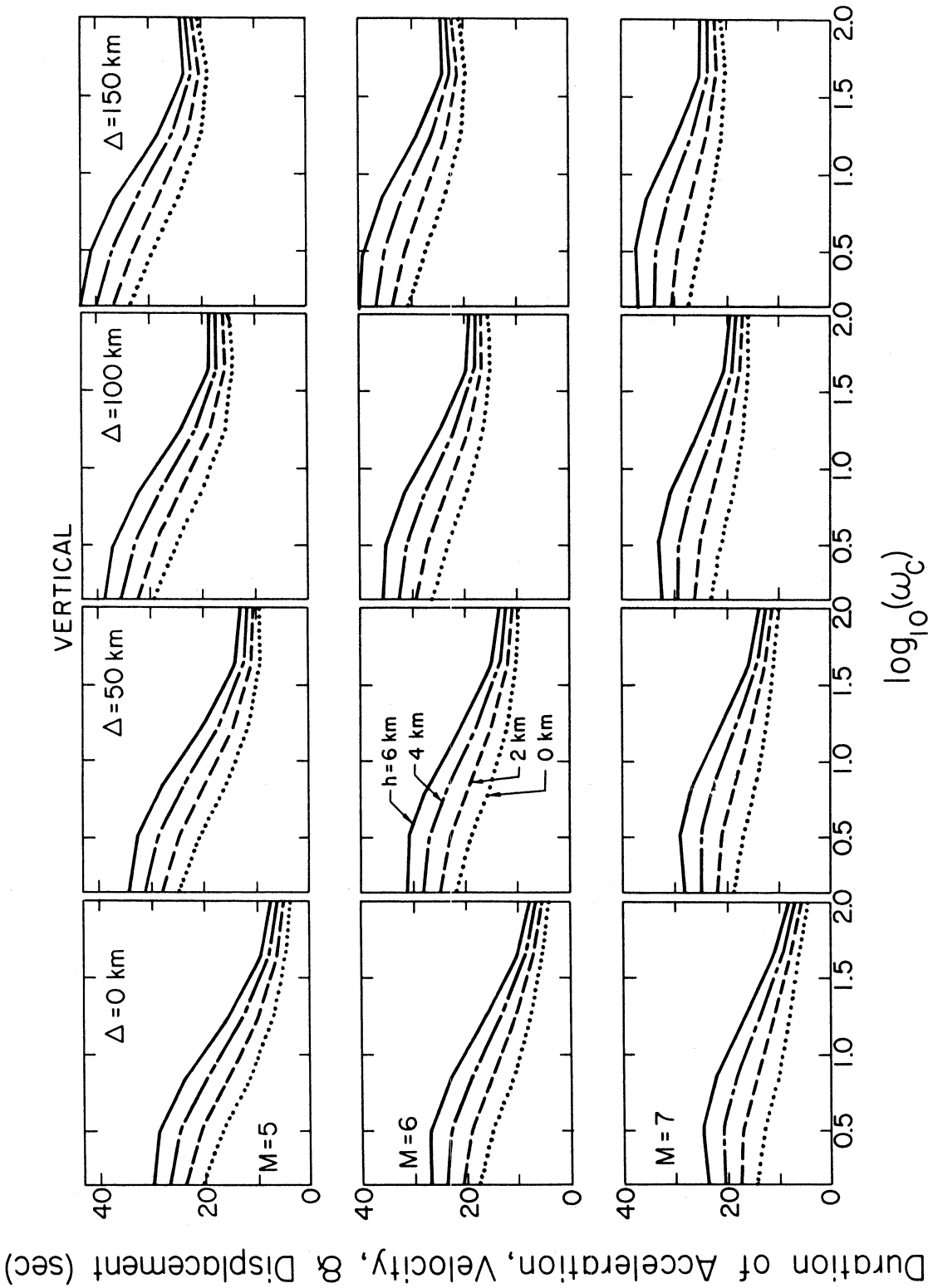


FIGURE 5a

The duration of strong vertical ground motion as calculated from equation (9) (with $\epsilon = 0$) versus frequency for selected magnitudes, epicentral distances, and the depths of sediments.

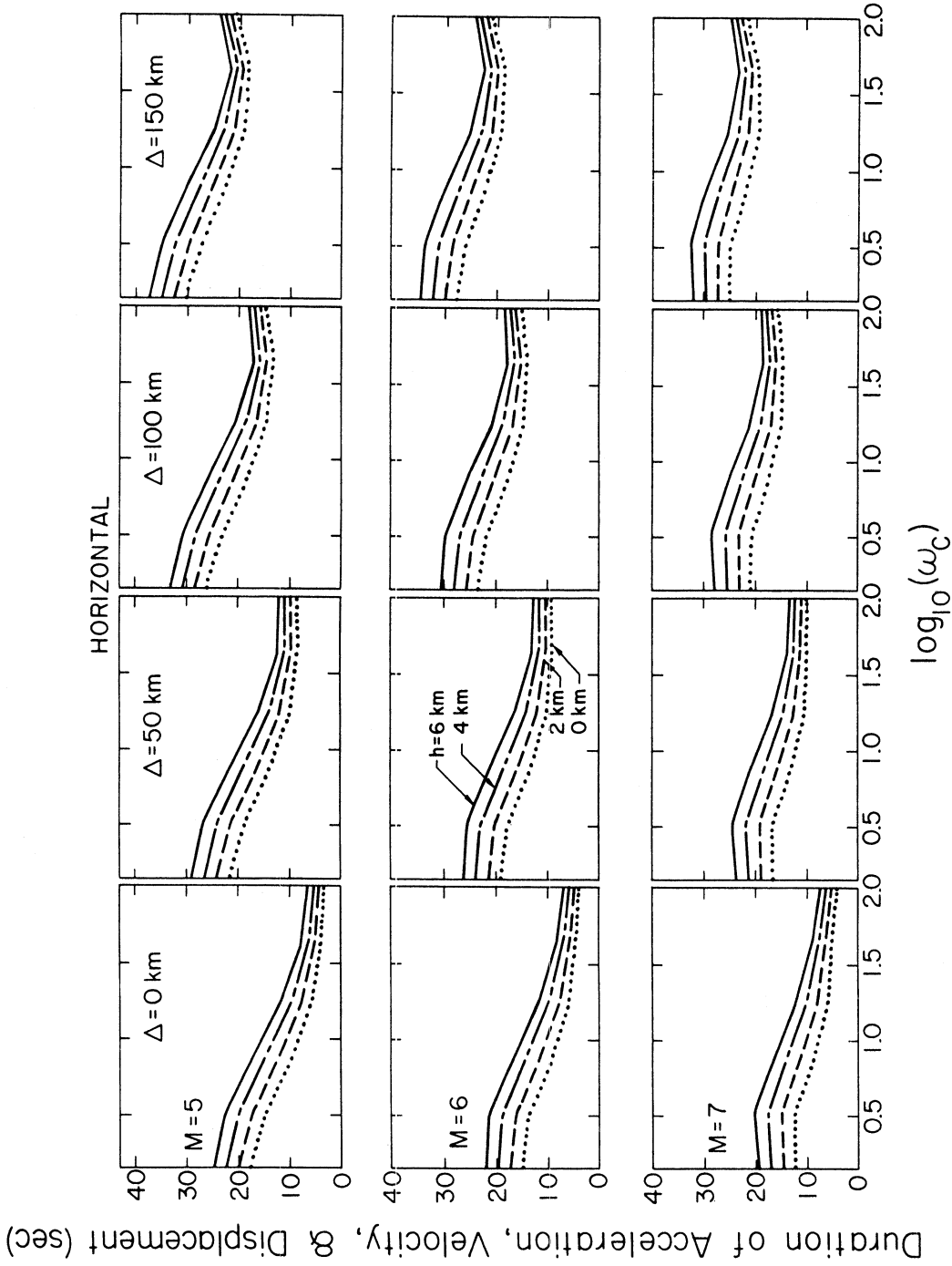


FIGURE 5b

The duration of strong horizontal ground motion as calculated from equation (9) (with $\epsilon = 0$) versus frequency for selected magnitudes, epicentral distances, and the depths of sediments.

$$\text{CORRELATIONS OF } \int_0^T a^2 dt, \int_0^T v^2 dt, \text{ AND } \int_0^T d^2 dt$$

WITH MAGNITUDE, EPICENTRAL DISTANCE, AND
DEPTH OF SEDIMENTS AT THE RECORDING SITE

For the correlations of the integrals of acceleration, velocity and displacement squared with the magnitude, epicentral distance, and depth of sediments for the six frequency bands, the following linear equation was used,

$$\log_{10} \int_0^T \begin{Bmatrix} a^2 \\ v^2 \\ d^2 \end{Bmatrix} dt = a(\omega_c) + b(\omega_c)M + c(\omega_c)M^2 + d(\omega_c)\Delta + e(\omega_c)h \\ + f(\omega_c)h^2 + g(\omega_c) \log_{10} A_0(\Delta). \quad (13)$$

a, b, c, d, e, f, and g are functions of the center frequencies of the six frequency bands and of the component (horizontal or vertical) of motion. The same functional dependence of the integrals on the magnitude and epicentral distance was adopted as in our previous study (Trifunac and Westermo, 1976a) since in this report we are concerned only with the refinement in the site classification term.

The magnitude dependent terms, $b(\omega_c)M + c(\omega_c)M^2$, in equation (13) are chosen to model the diminishing growth of these integrals as discussed by Trifunac (1976a,b) and Trifunac and Westermo (1976a). The values of $b(\omega_c)$ and $c(\omega_c)$ obtained from the regression show that $bM + cM^2$ increases with magnitude for $M < M_{\max}$, where

$$M_{\max} = - \frac{c(\omega_c)}{2b(\omega_c)}. \quad (14)$$

The decay of the integrals with increasing magnitude for $M > M_{\max}$ is not physically acceptable (Trifunac and Westermo, 1976a). Thus, for

$M > M_{\max}$ it is assumed that $bM + cM^2$ can be replaced by $bM_{\max} + cM_{\max}^2$.

The terms $d(\omega_c)\Delta + g(\omega_c) \log_{10} A_0(\Delta)$, represent the combination of geometrical and anelastic attenuation of the wave amplitudes with epicentral distance Δ where $A_0(\Delta)$ is a smoothed version of the empirically determined function (Richter, 1958) which describes the attenuation of wave amplitudes with distance in California. Table III lists the values of $A_0(\Delta)$ used in this study.

The functional dependence of the integrals $\int_0^T \{a^2, v^2, d^2\} dt$ on the depth of sediments at the recording site is not well understood. However, as mentioned previously, it is expected that these effects become small for depths shorter than the wavelengths $\lambda = \frac{2\pi}{\omega_c} \beta$ where β is the representative wave velocity. For a large enough depth, the contributions to the integrals from the multiple bottom reflections become negligible due to the anelastic attenuation. Between these limiting cases, multiple reflections off the bottom of the layer contribute to the integrals by means of the horizontally guided energy. A quadratic dependence on the depth of sediments, $e(\omega_c)h + f(\omega_c)h^2$ in equation (13), was chosen to model these expected trends. The variance of the coefficients $e(\omega_c)$ and $f(\omega_c)$ derived from the data showed them to be significantly different from zero at the 95% confidence level for all but the two highest frequency bands ($f_c = 18.0$ and 7.0 Hz). A different functional dependence of these integrals on the depth was also considered by combining it with a dependence on the epicentral distance and depth of the form $e'(\omega_c)h\Delta + f'(\omega_c)h^2\Delta$. The coefficients $e'(\omega_c)$ and $f'(\omega_c)$ were also found to be significantly different from zero at the 95% confidence level.

TABLE III

$\log_{10} A_o(\Delta)$ Versus Epicentral Distance Δ
(only the first two digits may be assumed to be significant)

| Δ (km) | $-\log_{10} A_o(\Delta)$ | Δ (km) | $-\log_{10} A_o(\Delta)$ | Δ (km) | $-\log_{10} A_o(\Delta)$ |
|------------------|--------------------------|------------------|--------------------------|------------------|--------------------------|
| 0 | 1.400 | 140 | 3.230 | 370 | 4.336 |
| 5 | 1.500 | 150 | 3.279 | 380 | 4.376 |
| 10 | 1.605 | 160 | 3.328 | 390 | 4.414 |
| 15 | 1.716 | 170 | 3.378 | 400 | 4.451 |
| 20 | 1.833 | 180 | 3.429 | 410 | 4.485 |
| 25 | 1.955 | 190 | 3.480 | 420 | 4.518 |
| 30 | 2.078 | 200 | 3.530 | 430 | 4.549 |
| 35 | 2.199 | 210 | 3.581 | 440 | 4.579 |
| 40 | 2.314 | 220 | 3.631 | 450 | 4.607 |
| 45 | 2.421 | 230 | 3.680 | 460 | 4.634 |
| 50 | 2.517 | 240 | 3.729 | 470 | 4.660 |
| 55 | 2.603 | 250 | 3.779 | 480 | 4.685 |
| 60 | 2.679 | 260 | 3.827 | 490 | 4.709 |
| 65 | 2.746 | 270 | 3.877 | 500 | 4.732 |
| 70 | 2.805 | 280 | 3.926 | 510 | 4.755 |
| 80 | 2.920 | 290 | 3.975 | 520 | 4.776 |
| 95 | 2.958 | 300 | 4.024 | 530 | 4.797 |
| 90 | 2.989 | 310 | 4.072 | 540 | 4.817 |
| 95 | 3.020 | 320 | 4.119 | 550 | 4.835 |
| 100 | 3.044 | 330 | 4.164 | 560 | 4.853 |
| 110 | 3.089 | 340 | 4.209 | 570 | 4.869 |
| 120 | 3.135 | 350 | 4.253 | 580 | 4.885 |
| 130 | 3.182 | 360 | 4.295 | 590 | 4.900 |

Although this and probably other functional forms could not be rejected at the 95% confidence level, we chose to examine the dependence of these integrals on the depth of sediments in terms of the simple equation (13) only.

If it is assumed that each frequency band is sufficiently narrow the following approximate relations hold,

$$\begin{aligned} |v(t)| &\approx |\omega_c d(t)| \\ |a(t)| &\approx |\omega_c v(t)| \quad , \end{aligned} \quad (15)$$

and thus

$$\begin{aligned} \log_{10} \int_0^T d^2 dt &\approx \log_{10} \int_0^T a^2 dt - 4 \log_{10} \omega_c \\ \log_{10} \int_0^T v^2 dt &\approx \log_{10} \int_0^T a^2 dt - 2 \log_{10} \omega_c \quad . \end{aligned} \quad (16)$$

To expand the data base for the correlations, the data for $\log_{10} \int_0^T v^2 dt$ and $\log_{10} \int_0^T d^2 dt$ were "corrected" by means of equation (16) and applied to equation (13) in regression analysis on $\log_{10} \int_0^T a^2 dt$. Equation (16) is then used to modify the coefficient $a(\omega_c)$ in equation (13) for $\log_{10} \int_0^T \left\{ \frac{v^2}{d^2} \right\} dt$. The same regressional procedure was used here as in the previous section, and the residual, ϵ , was calculated as a function of the confidence level from

$$\begin{aligned} \epsilon_i &= \log_{10} \int_0^T a^2 dt - \{a + bM + cM^2 + d\Delta + eh + fh^2 \\ &\quad + g \log_{10} A_o(\Delta)\} \quad . \end{aligned} \quad (17)$$

A Gaussian distribution was fit to the data $p(\epsilon)$ as it has been noted that the distributions for models of the Fourier amplitude spectrum can

be approximated by a Gaussian distribution (Anderson and Trifunac, 1977). Figures 6a and 6b show the data $p(\epsilon_i)$, and the fitted Gaussian distribution for all six frequency bands and for both vertical and horizontal components of motion. The Kolmogorov-Smirnov test at the 95% confidence level was passed for all of the $p(\epsilon)$ functions. The Chi-Squared test failed at the 95% confidence level for only two of the twelve functions. Since both tests were passed for most of the frequency bands of each component of motion, a Gaussian distribution was assumed to be an acceptable approximation. The $p(\epsilon)$ distribution is then completely described by the mean, $\mu(\omega_c)$, and the standard deviation, $\sigma(\omega_c)$, of the Gaussian distribution given by

$$p(\epsilon) = \frac{1}{\sqrt{2\pi}} \int_{-\infty}^{\frac{\epsilon-\mu}{\sigma}} e^{-\frac{1}{2}x^2} dx \quad . \quad (18)$$

Table IV lists the coefficients a, b, c, d, e, f, and g, and the mean, μ , and standard deviation, σ , of the residuals along with the values of h_{\max} and M_{\max} for which the terms $eh + fh^2$ and $bM + cM^2$ reach their extrema. The coefficients are plotted versus the center frequency in Figures 7a and 7b.

The variation of $\log_{10} \int_0^T a^2 dt$ with the depth of sediments can be best seen from Figures 8a and 8b which are plots of $\log_{10} \int_0^T a^2 dt$ calculated from equation (13) with the coefficients smoothed along frequency axis by a $(\frac{1}{4}, \frac{1}{2}, \frac{1}{4})$ filter and plotted for various magnitudes, epicentral distances, depth of sediments, and for $\epsilon = 0$. The influence of the depth is quite apparent for the lower frequencies $f_c = 0.2, 0.5, \text{ and } 1.1$ Hz where the value of $\int_0^T a^2 dt$ can vary as much as one order of magnitude for

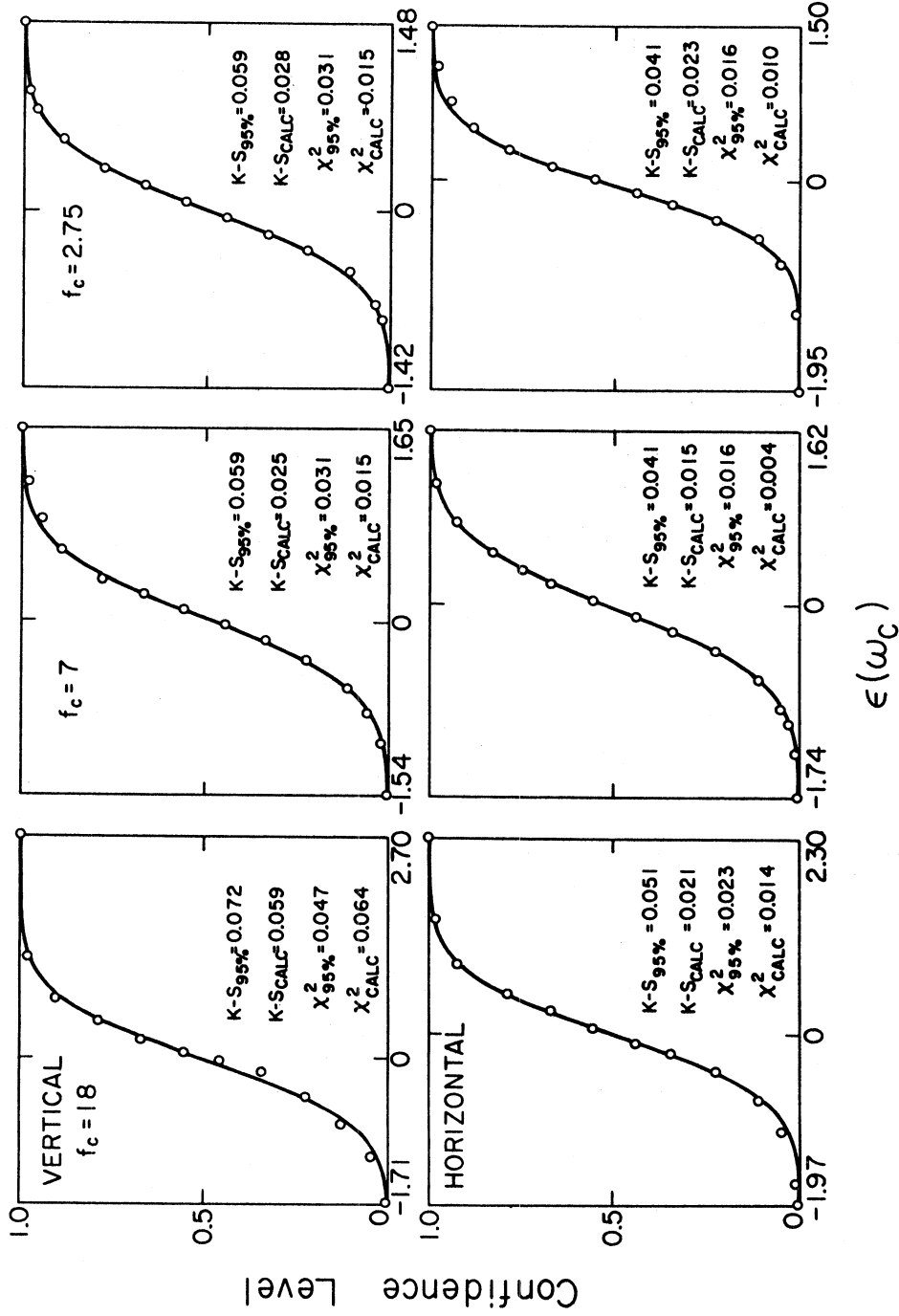
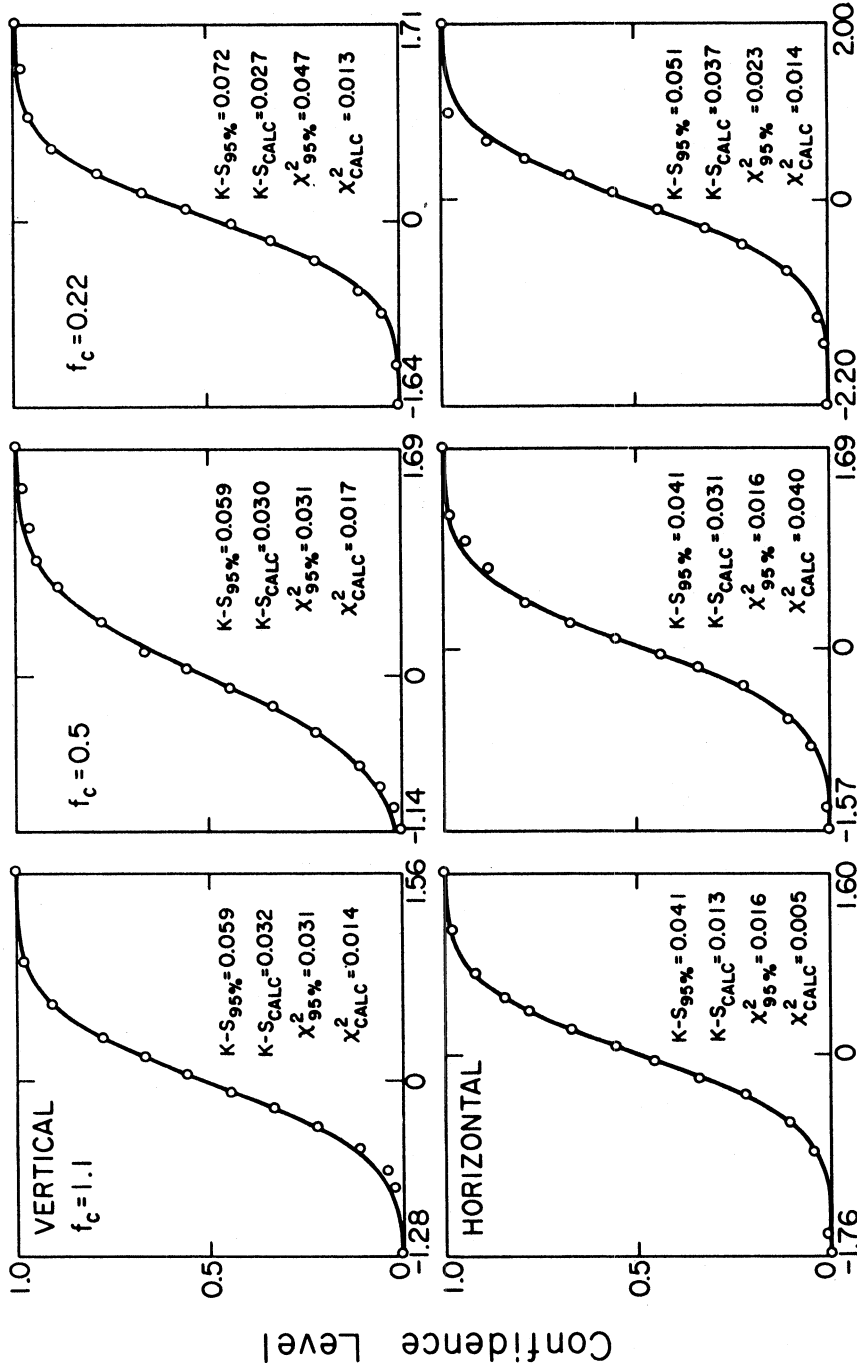


FIGURE 6a

The confidence level, p , versus the residual, ϵ , for the calculated residuals (circles) and for the fitted Gaussian distribution (solid curve). The Chi-Squared and Kolmogorov-Smirnov criteria are listed for each distribution.



$\epsilon(\omega_c)$

FIGURE 6b

The confidence level, p , versus the residual, ϵ , for the calculated residuals (circles) and for the fitted Gaussian distribution (solid curve). The Chi-Squared and Kolmogorov-Smirnov criteria are listed for each distribution.

TABLE IV

Regression Coefficients in

$$\log_{10} \int_0^T a^2(t) dt = a + bM + cM^2 + d\Delta + eh + fh^2 + g \log_{10} A_0(\Delta)$$

VERTICAL COMPONENT

| | $f_c = 18$ | $f_c = 7$ | $f_c = 2.75$ | $f_c = 1.1$ | $f_c = 0.5$ | $f_c = 0.22$ |
|-------------------|------------|-----------|--------------|-------------|-------------|--------------|
| a | -2.303 | -1.281 | -0.718 | -0.994 | -1.122 | -1.225 |
| Variance(a)(x0.1) | 0.111 | 0.065 | 0.057 | 0.062 | 0.062 | 0.104 |
| b | 7.887 | 4.588 | 2.917 | 3.579 | 3.740 | 3.718 |
| Variance(b) | 0.378 | 0.225 | 0.196 | 0.214 | 0.216 | 0.353 |
| c | -5.535 | -2.949 | -1.717 | -2.115 | -2.216 | -2.408 |
| Variance(c)(x10) | 0.321 | 0.192 | 0.167 | 0.183 | 0.184 | 0.299 |
| d | -1.051 | -1.013 | -0.452 | -0.141 | -0.111 | -0.610 |
| Variance(d)(x100) | 0.140 | 0.100 | 0.087 | 0.095 | 0.095 | 0.131 |
| e | -1.519 | -0.163 | 1.652 | 3.419 | 4.669 | 2.931 |
| Variance(e)(x10) | 0.384 | 0.271 | 0.236 | 0.258 | 0.259 | 0.358 |
| f | 1.928 | 0.014 | -2.924 | -5.365 | -6.640 | -3.548 |
| Variance(f)(x100) | 0.676 | 0.477 | 0.415 | 0.453 | 0.456 | 0.630 |
| g | 8.409 | 3.983 | 5.725 | 8.215 | 7.720 | 0.333 |
| Variance(g)(x10) | 1.433 | 1.025 | 0.892 | 0.975 | 0.981 | 1.336 |
| μ (x100) | 0.500 | -0.600 | -0.930 | -1.390 | -2.000 | -0.200 |
| σ (x10) | 6.133 | 4.932 | 4.372 | 4.414 | 5.381 | 4.830 |
| M_{\max} | 7.124 | 7.780 | 8.493 | 8.459 | 8.437 | 7.721 |
| h_{\max} | 3.939 | 60.350 | 2.825 | 3.187 | 3.516 | 4.131 |
| No. of Data | 360 | 540 | 540 | 540 | 540 | 360 |

TABLE IV

(Continued)

HORIZONTAL COMPONENT

| | $f_c = 18$ | $f_c = 7$ | $f_c = 2.75$ | $f_c = 1.1$ | $f_c = 0.5$ | $f_c = 0.22$ |
|-------------------------------|-----------------|-----------------|-----------------|-----------------|-----------------|-----------------|
| a | | | | | | |
| Variance(a) ^(x0.1) | -1.696 0.111 | -0.862 0.065 | -0.428 0.057 | -0.420 0.062 | -0.546 0.062 | -0.929 0.104 |
| b | | | | | | |
| Variance(b) | 5.687 0.378 | 3.329 0.225 | 2.209 0.196 | 1.967 0.214 | 1.992 0.216 | 2.709 0.353 |
| c | | | | | | |
| Variance(c) ^(x10) | -3.792 0.321 | -1.893 0.192 | -1.105 0.167 | -0.795 0.183 | -0.684 0.184 | -1.448 0.299 |
| d | | | | | | |
| Variance(d) ^(x100) | -1.286 0.140 | -1.092 0.100 | -0.487 0.087 | 0.003 0.095 | 0.200 0.095 | -0.631 0.131 |
| e | | | | | | |
| Variance(e) ^(x10) | 0.201 0.384 | 0.330 0.271 | 1.558 0.236 | 3.558 0.258 | 5.450 0.259 | 6.119 0.358 |
| f | | | | | | |
| Variance(f) ^(x100) | -1.082 0.676 | -0.769 0.477 | -2.087 0.415 | -4.756 0.453 | -6.875 0.456 | -7.929 0.630 |
| g | | | | | | |
| Variance(g) ^(x10) | 5.127 1.433 | 4.205 1.025 | 6.707 0.892 | 9.847 0.975 | 10.682 0.981 | 1.232 1.336 |
| μ (x100) | 0.801 | -0.350 | -1.010 | 0.300 | -0.760 | 2.090 |
| σ (x10) | 5.883 | 5.360 | 4.291 | 4.854 | 4.875 | 6.122 |
| M_{\max} | 7.500 | 8.790 | 9.995 | 12.370 | 14.563 | 9.355 |
| h_{\max} | 0.930 | 2.148 | 3.734 | 3.741 | 3.963 | 3.859 |
| No. of Data | 720 | 1080 | 1080 | 1080 | 1080 | 720 |

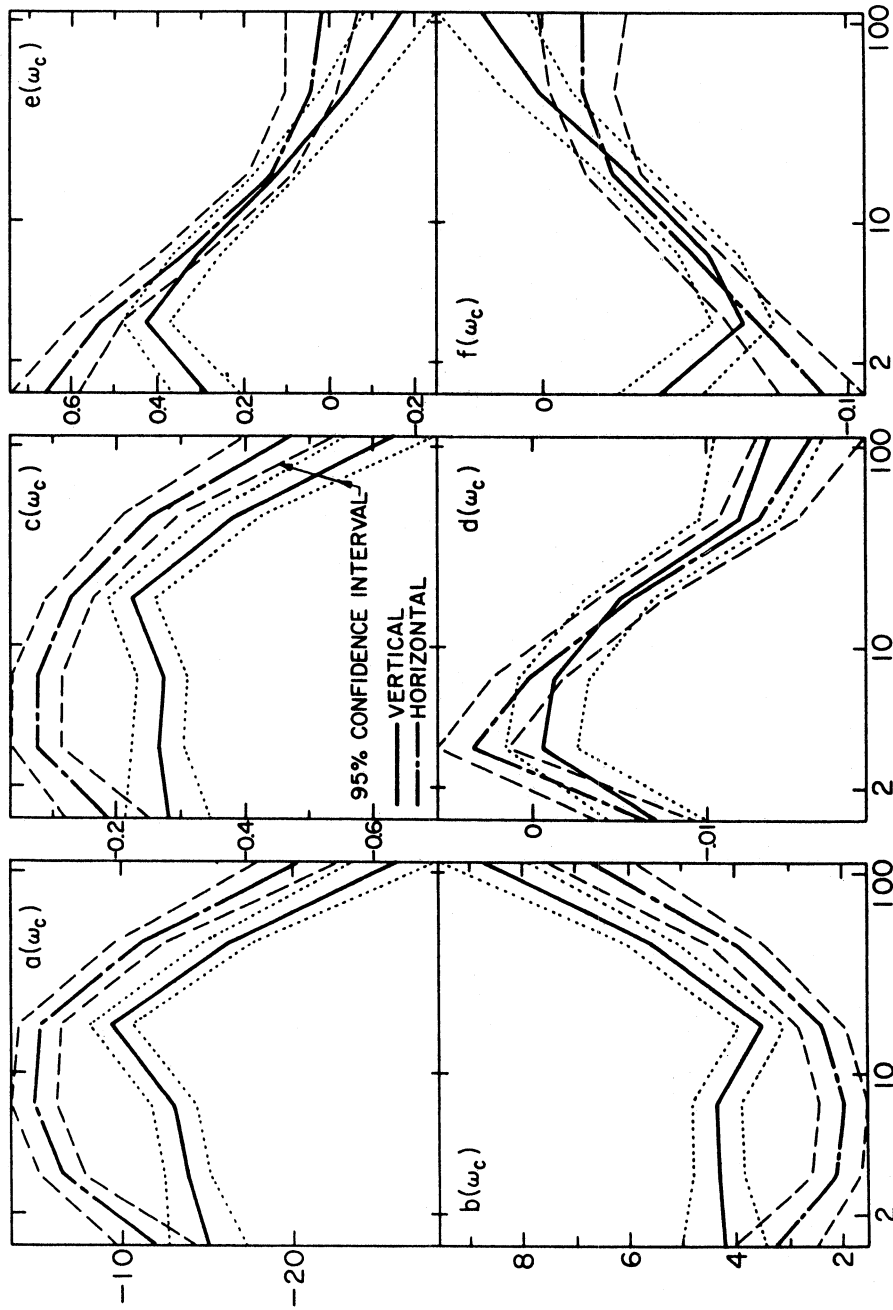
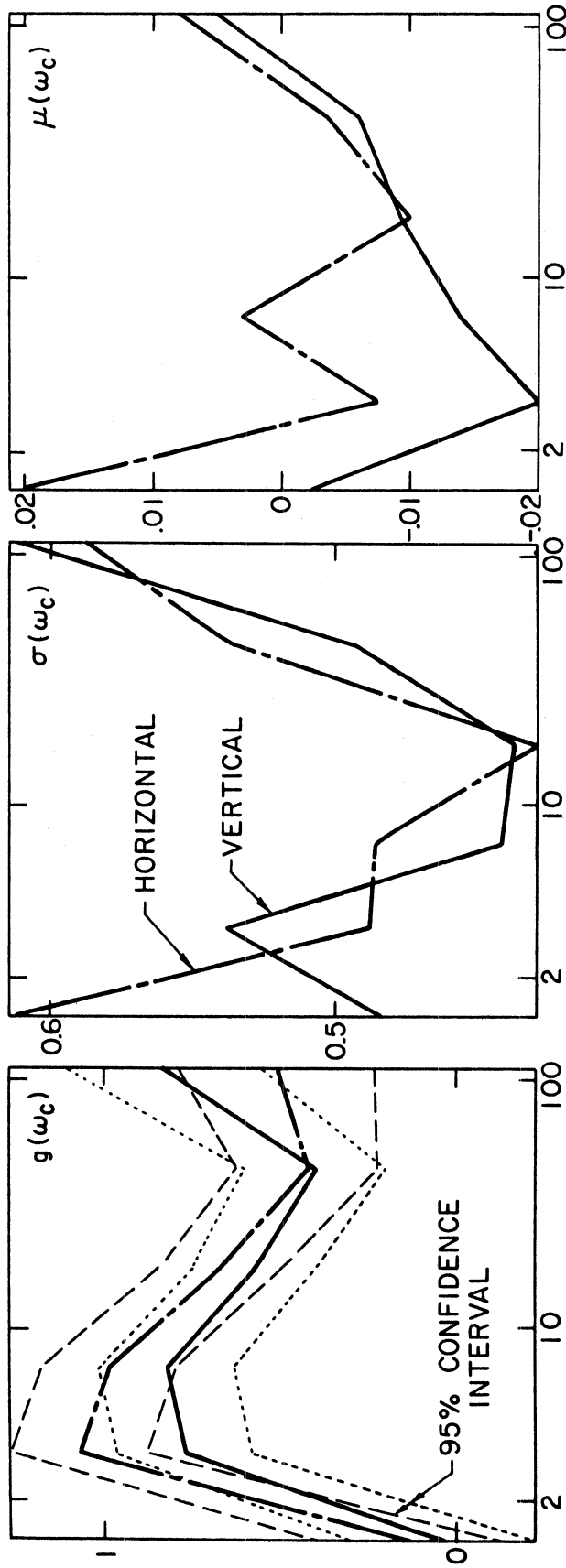
Center Frequency ω_c , rad/sec

FIGURE 7a

The coefficients a, b, c, d, e, and f in equation (13) for horizontal and vertical motions plotted versus $\omega_c = 2\pi f_c$ (for $f_c = 0.22, 0.5, 1.1, 2.75, 7.0$ and 18.0 Hz). The coefficients are bounded by the calculated 95% confidence interval.



Center Frequency ω_c , rad/sec

FIGURE 7b

The coefficients g , μ , and σ in equations (13) and (18) for horizontal and vertical components of motion plotted versus $\omega_c = 2\pi f_c$ (for $f_c = 0.22, 0.5, 1.1, 2.75, 7.0$ and 18.0 Hz). $g(\omega_c)$ is bounded by the calculated 95% confidence interval.

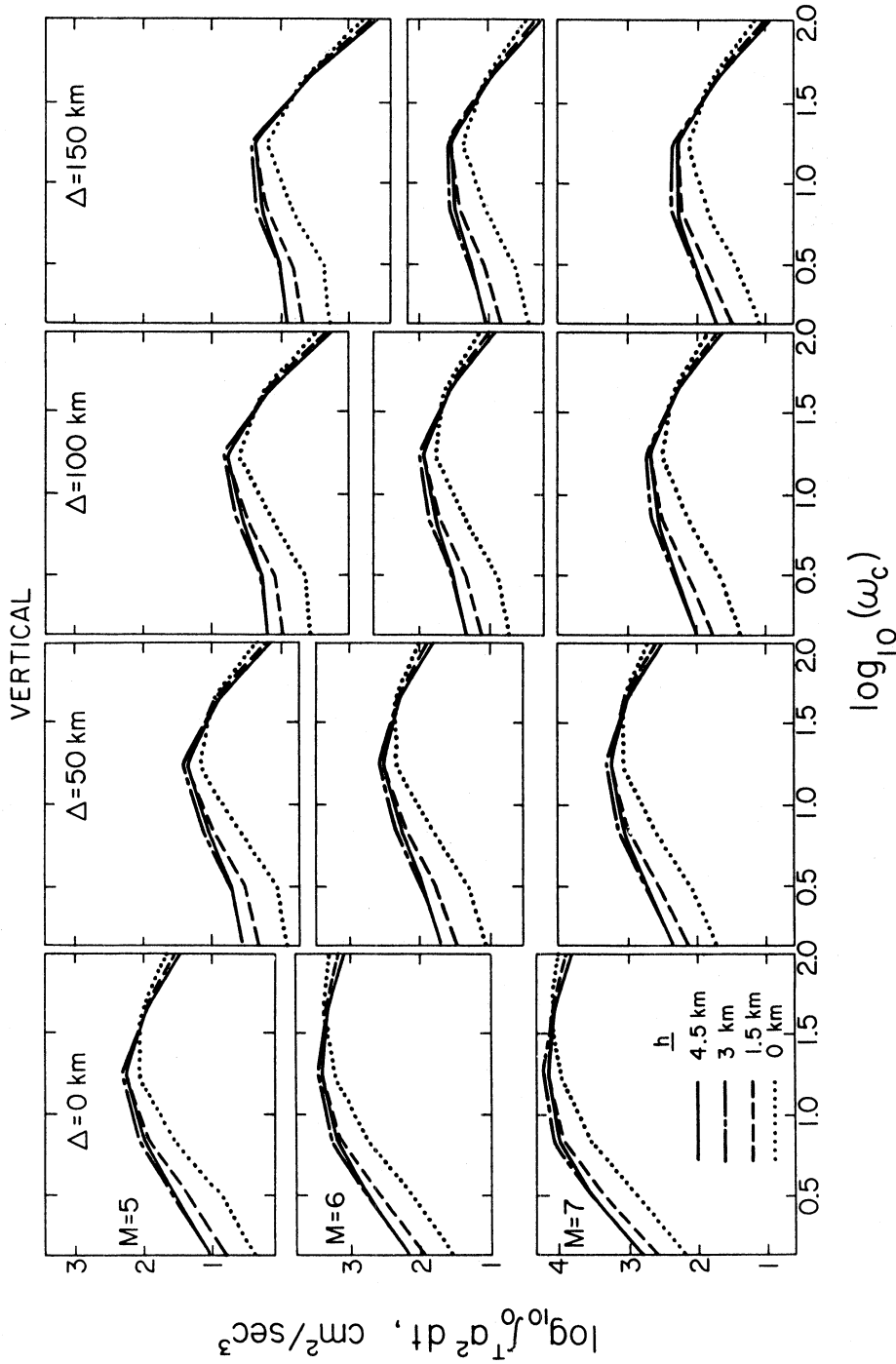
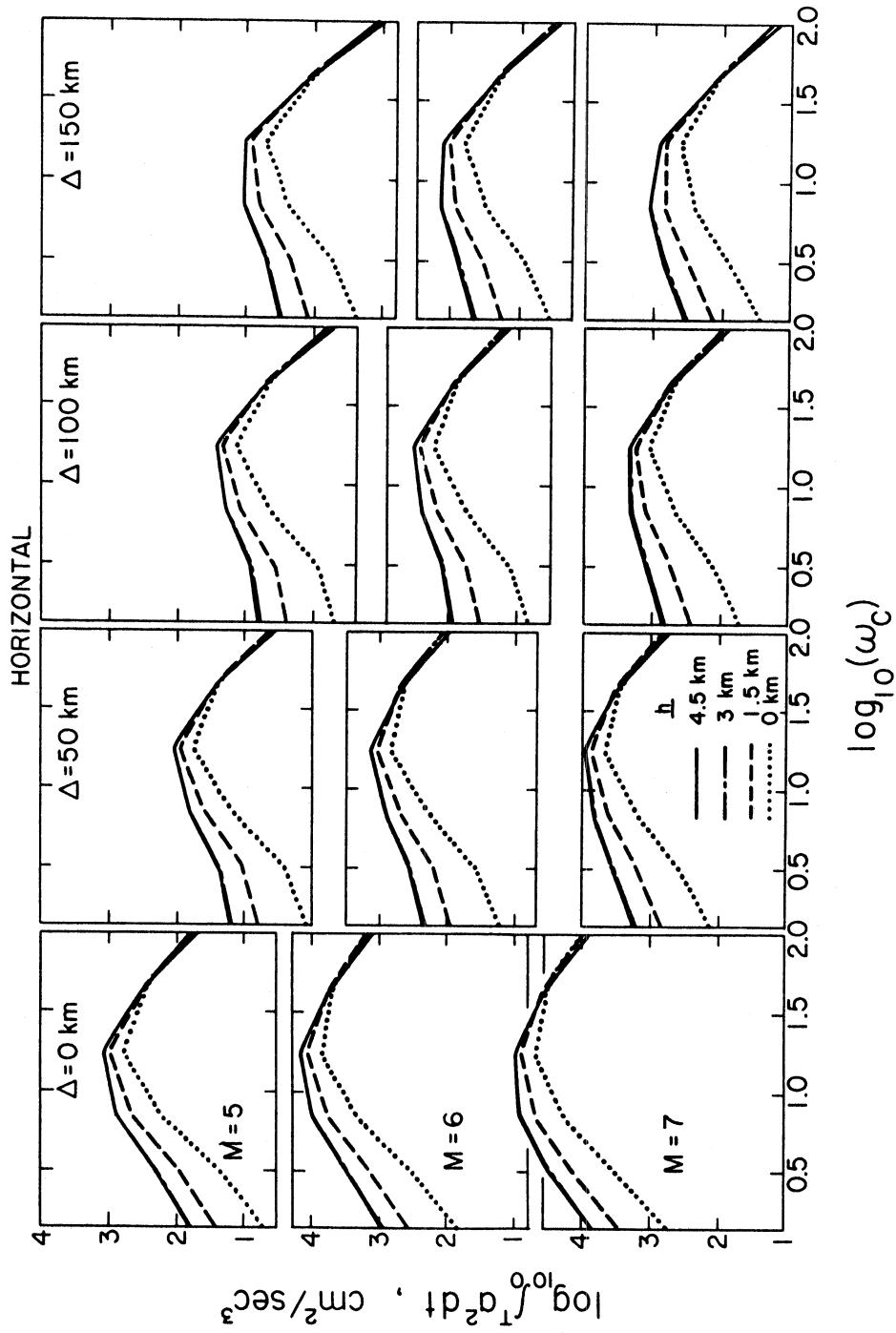


FIGURE 8a

The amplitudes of $\log_{10} \int_0^T a^2(t) dt$ computed from equation (13) (with $\epsilon = 0$) for vertical motion versus frequency for selected magnitudes, epicentral distances, and depth of sediments.



The amplitudes of $\log_{10} \int_0^T a^2(t) dt$ computed from equation (13) (with $\epsilon = 0$) for horizontal motion versus frequency for selected magnitudes, epicentral distances, and depth of sediments.

$h = 0$ compared to $h = 4$ km. For the two highest frequency bands, $f_c = 18.0$ and 7.0 Hz, $\int_0^T a^2 dt$ decreases slightly with increasing depth.

Figure 9 is a plot of the depth dependent terms in equation (13); $e(\omega_c)h + f(\omega_c)h^2$. For the smoothed coefficients at the two highest frequency bands, $f_c = 18.0$ and 7.0 Hz, one or both of the components of this depth dependent term indicate that the values of $\int_0^T a^2 dt$ decrease with increasing depth. However, for these two frequency bands, both $e(\omega_c) = 0$ and $f(\omega_c) = 0$ lie within the 95% confidence interval. Thus, the scatter of the data is too large to allow any conclusions as to whether or not the integrals actually do decrease with increasing depth for high frequencies. The maxima of the terms, $eh + fh^2$, for the four lowest frequency bands lie consistently in the 3 to 4 km depth range. These peaks however may not be significant since 82% of the depth data is for a depth of less than 4 km. Whether $\int_0^T a^2 dt$ increases still further or indeed begins to decrease for depths beyond 4 km can only be answered when strong motion records for sites with greater depths of sediments become available.

The contribution to $\log_{10} \int_0^T a^2 dt$ from the terms involving the earthquake magnitude, as given by $b(\omega_c)M + c(\omega_c)M^2$ in equation (13), is plotted versus magnitude in Figure 9. From this figure it is seen that the trend is for the integrals to increase with increasing magnitude up to $M = M_{\max}$, as noted in our previous correlations of $\int_0^T a^2 dt$ with the earthquake magnitude. Since the present equation (13) involves only a revision of the site geology effects, it would be expected that there is little difference between the magnitude dependent coefficients of these two

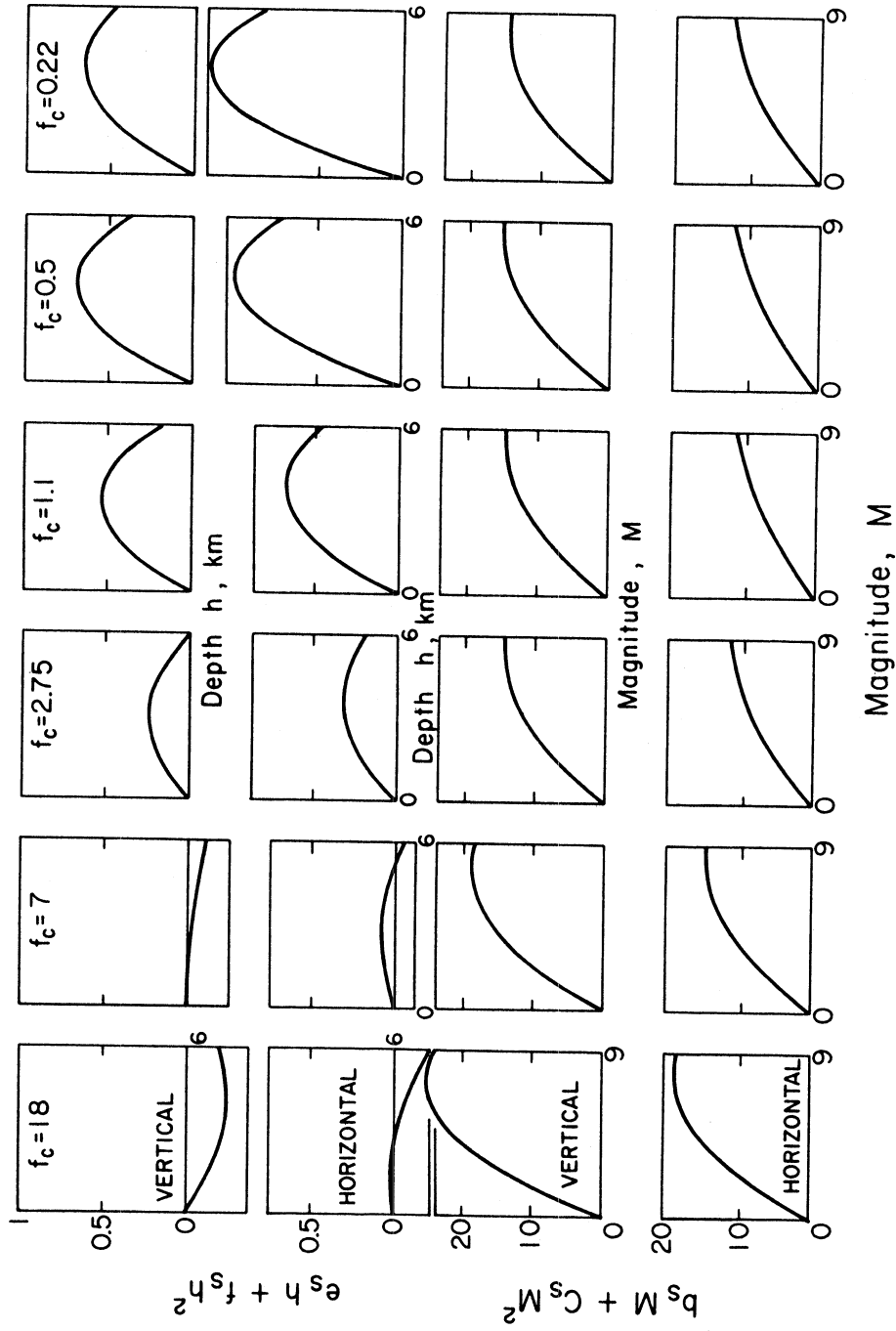


FIGURE 9

Amplitudes of $eh + fh^2$ (top) and $bM + cM^2$ (bottom) versus depth, h , and magnitude, M , respectively, in terms of the frequency smoothed coefficients.

correlations. However, a comparison of Figure 6 in Trifunac and Westermo (1976a) and Figure 6 in this report shows that for the lower frequencies ($f_c = 2.75, 1.1, 0.5$ and 0.2 Hz) the values of M_{\max} are larger for this study than those found previously. This difference in the M_{\max} 's is largest for the horizontal component and $f_c = 0.5$ Hz band where we had previously found $M_{\max} = 7.53$ compared to the present value of $M_{\max} = 14.56$. This shift in M_{\max} is due to the correlation of the site effects in terms of the depth of sediments instead of the site classification, s , and lies in the fact that the depths used in the data are unevenly distributed in the magnitude range. For the magnitude range of $M = 4$ to $M = 5$, the mean depth is 1.16 km, for $M = 5$ to $M = 6$, the mean depth is 1.66 km, and for $M = 6$ to $M = 7$, the mean depth is 2.47 km. Since the larger magnitude records had a larger mean recording site depth for the available data, and since the integrals tend to increase with increasing depth, the regression of equation (13) may have "interpreted" the growth of the integrals with depth, at large depths, as partly due to a growth with magnitude increasing beyond $M = 7$. This effect seems to be more prominent for the horizontal component of motion and for low frequencies ($f_c = 1.1, 0.5$ and 0.2 Hz) where the increase of the integrals with the depth and M_{\max} are the largest.

Although the 95% confidence interval of the coefficient $c(\omega_c)$ in Figure 7a includes zero at $f_c = 1.1$ and 0.5 Hz, the term $c(\omega_c)\Delta$ was included in equation (13) to account for anelastic attenuation of the form, $e^{-\omega\Delta/2Q\beta}$. Since the term $g(\omega_c)\log_{10}A_0(\Delta)$ is also included in the model equation as a function of frequency, the coefficient $c(\omega_c)$ is essentially

a frequency dependent correction term to the $\log_{10} A_0(\Delta)$ attenuation that includes the anelastic attenuation. From Figures 7a and 7b, it is seen that at the center frequencies $f_c = 0.5$ and 1.1 Hz, where $c(\omega_c)$ is small, the coefficient $g(\Delta_c)$ is at a relative maximum. This suggests that the empirically derived $A_0(\Delta)$ function represents the average combination of geometrical spreading and anelastic attenuation in California for the frequency range around 1.0 Hz (Trifunac, 1976b).

The values of the integrals are most strongly influenced by the epicentral distance in the highest frequency range, $f_c = 18.0$ Hz as shown in Figures 8a and 8b. At this frequency, $\int_0^T a^2 dt$ decreases by about three orders of magnitude in going from a zero epicentral distance to $\Delta = 150$ km for both components of motion. The low frequency integrals ($f_c = 0.22$ Hz) only decrease by approximately 1.5 orders of magnitude for the horizontal motion and 1.0 order of magnitude for the vertical motion for the same range of epicentral distance ($\Delta = 0$ km to $\Delta = 150$ km).

CORRELATIONS OF $\int_0^T \begin{Bmatrix} a^2 \\ v^2 \\ d^2 \end{Bmatrix} dt/\text{Duration}$ WITH
EARTHQUAKE MAGNITUDE, EPICENTRAL DISTANCE, AND DEPTH OF SEDIMENTS

The average rate (Trifunac and Westermo, 1976a) as defined by

$$\text{Rate} \begin{Bmatrix} a \\ v \\ d \end{Bmatrix} = \int_0^T \begin{Bmatrix} a^2 \\ v^2 \\ d^2 \end{Bmatrix} dt/\text{Duration} \begin{Bmatrix} a \\ v \\ d \end{Bmatrix} \quad (19)$$

can be calculated from the correlations of the previous two sections. However, to avoid the compounded error and the inherent mixing of the functional terms in dividing the two equations, new direct regressions of the average rate with the magnitude, epicentral distance, and the depth of sediments at the recording site were performed in terms of the following equation,

$$\log_{10} \left[\int_0^T \begin{Bmatrix} a^2 \\ v^2 \\ d^2 \end{Bmatrix} dt/\text{Duration} \right] = a(\omega_c) + b(\omega_c)M + c(\omega_c)M^2 \\ + d(\omega_c)\Delta + e(\omega_c)h + f(\omega_c)h^2 + g(\omega_c)\log_{10}A_o(\Delta) \quad (20)$$

The above equation is identical to the model equation in Trifunac and Westermo (1976a) except that the site classification term has been replaced by $e(\omega_c)h + f(\omega_c)h^2$. The data used in the regression of equation (20) was identical to that used in the previous sections. Here also, the frequency bands were assumed narrow enough that equations (10) and (16) yield

$$\log_{10}\text{Rate}(d) \approx \log_{10}\text{Rate}(a) - 4 \log_{10}\omega_c , \\ \log_{10}\text{Rate}(v) \approx \log_{10}\text{Rate}(a) - 2 \log_{10}\omega_c . \quad (21)$$

The velocity and displacement data were modified by equation (21) and

combined with the acceleration data.

The residual, ϵ , defined by

$$\epsilon_i = \log_{10} \left[\int_0^T a^2 dt / \text{Duration} \right] - \{ a + bM + cM^2 + d\Delta + eh + fh^2 + g \log_{10} A_o(\Delta) \} , \quad (22)$$

was calculated as a function of the confidence level, p , and is shown in Figures 10a and 10b. A trial Gaussian distribution was fitted to each of these functions, $p(\epsilon)$, and it passed the 95% Kolmogorov-Smirnov test for all of the frequency bands and failed the 95% Chi-Squared test for only one frequency band. Table V lists the values of a , b , c , d , e , f , and g resulting from the regression of equation (20) with the data and the values of μ and σ from fitting a Gaussian distribution (given by equation (18)) to the $p(\epsilon_i)$ data. These coefficients are shown plotted versus frequency in Figures 11a and 11b along with their 95% confidence intervals.

The standard deviations of the residual, $\sigma(\omega_c)$, are greatest for both the highest and the lowest frequency bands ($f_c = 18.0$ and 0.22 Hz, respectively), with 68% of the data varying by less than a factor of 5 at these frequencies. The general trend of the coefficients with the frequency is very similar to the behavior of the coefficients for the correlation with the integral of the a , v and d functions squared (Figures 7a and 7b). The standard deviations of the residuals for these correlations are larger than the standard deviations for the correlations of the integrals by approximately 0.1 (on the logarithmic scale).

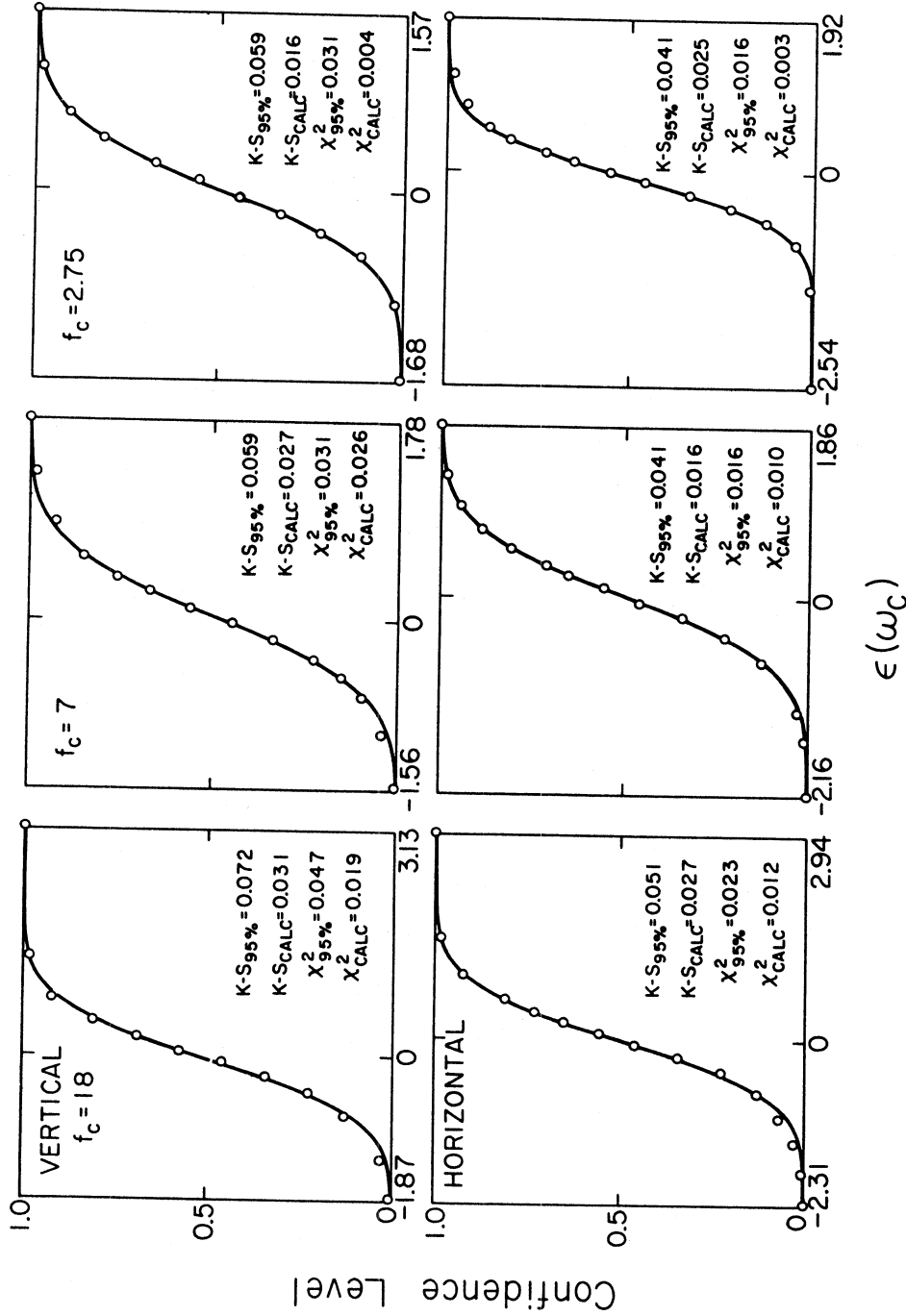


FIGURE 10a

The confidence level, p , versus the residual, ϵ , for the calculated residuals (circles) and for the fitted Gaussian distribution (solid curve). The Chi-Squared and Kolmogorov-Smirnov criteria are listed for each distribution.

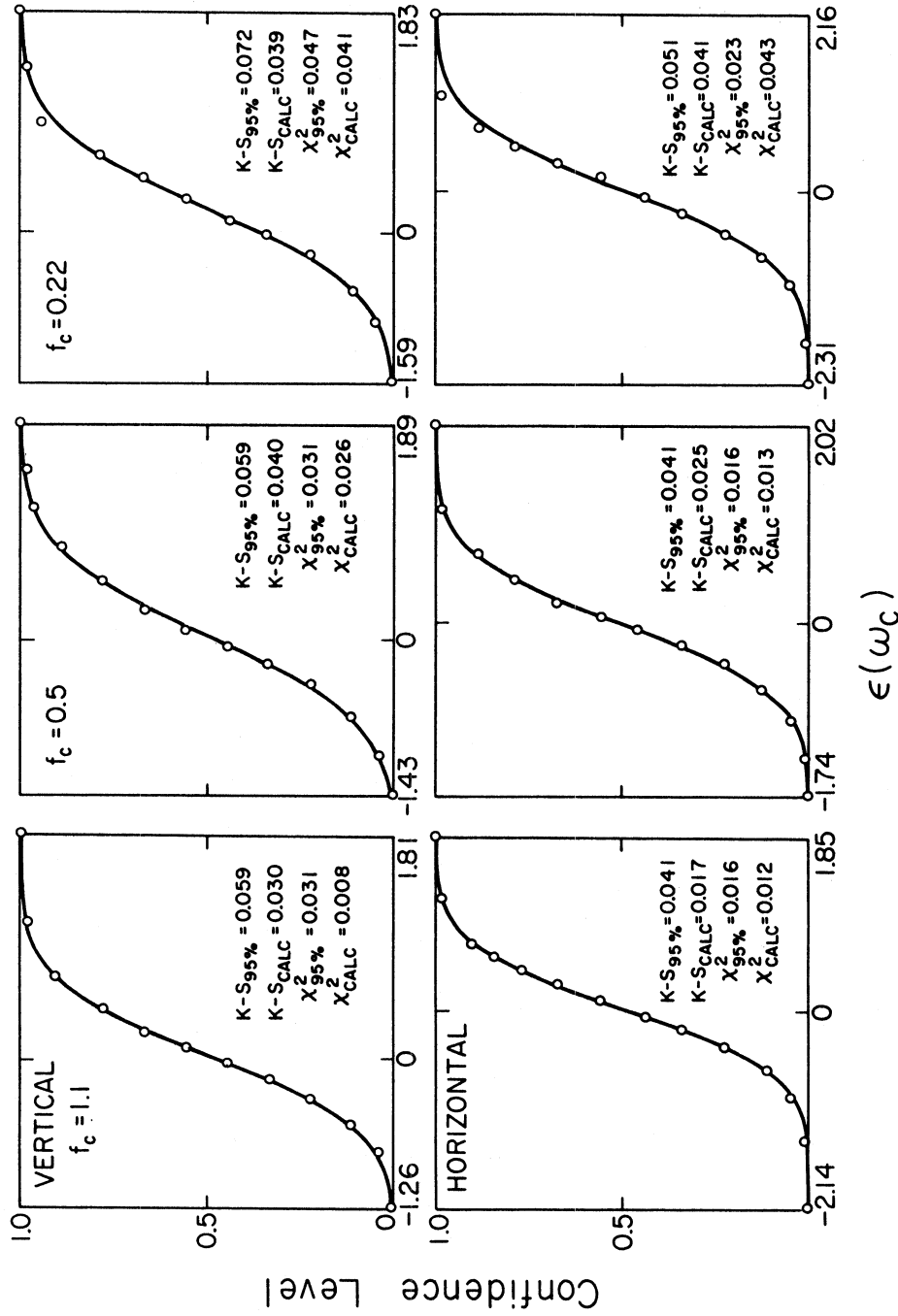


FIGURE 10b

The confidence level, p , versus the residual, ϵ , for the calculated residuals (circles) and for the fitted Gaussian distribution (solid curve). The Chi-Squared and Kolmogorov-Smirnov criteria are listed for each distribution.

TABLE V

Regression Coefficients in

$$\log_{10} \left[\int_0^T a^2(t) dt / \text{Duration} \right] = a + bM + cM^2 + d\Delta + eh + fh^2 + g \log_{10} A_0(\Delta)$$

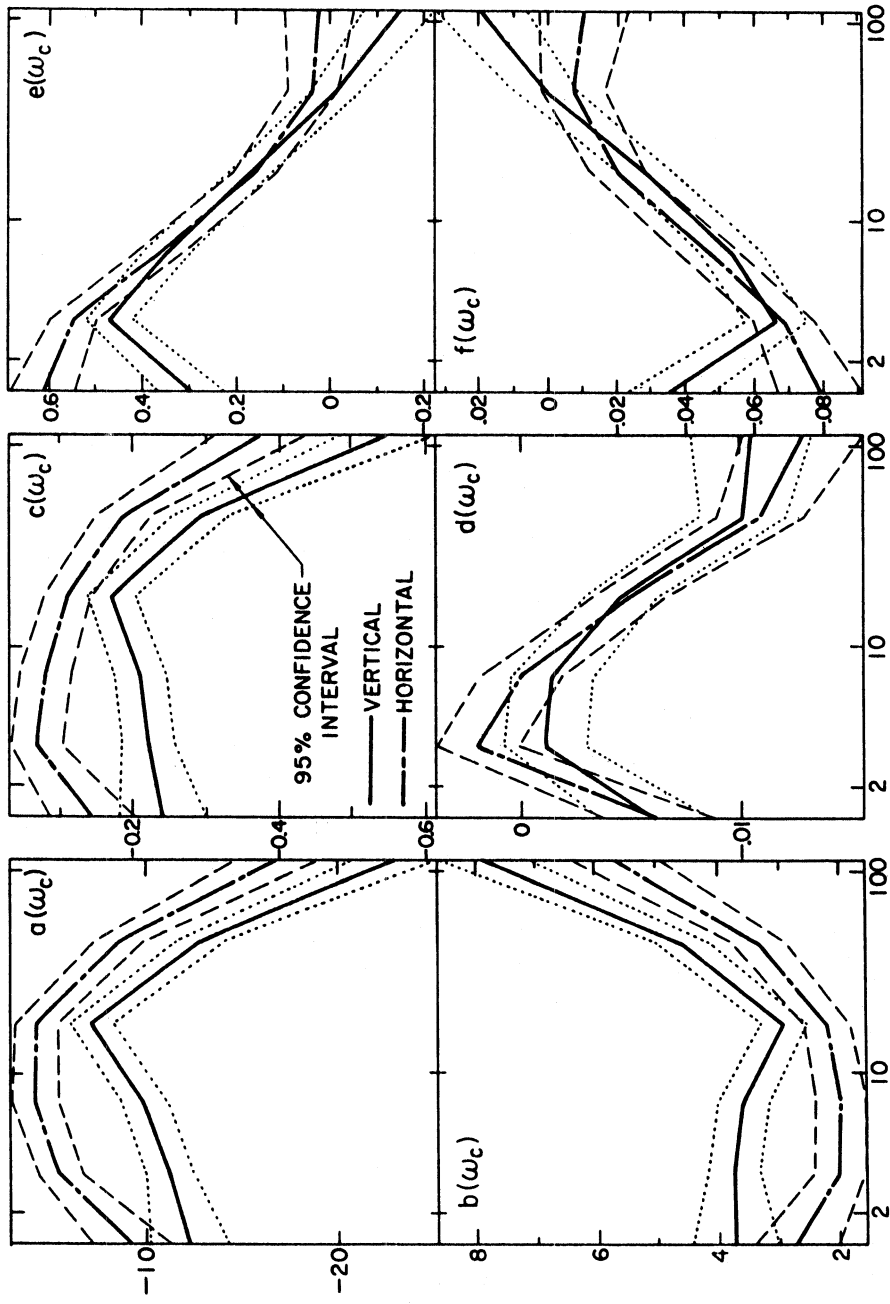
VERTICAL COMPONENT

| | $f_c = 18$ | $f_c = 7$ | $f_c = 2.75$ | $f_c = 1.1$ | $f_c = 0.5$ | $f_c = 0.22$ |
|-------------------|------------|-----------|--------------|-------------|-------------|--------------|
| a | -2.613 | -1.611 | -0.940 | -1.300 | -1.378 | -1.498 |
| Variance(a)(x0.1) | 0.125 | 0.074 | 0.064 | 0.067 | 0.068 | 0.117 |
| b | 8.751 | 5.534 | 3.501 | 4.343 | 4.296 | 4.209 |
| Variance(b) | 0.425 | 0.258 | 0.222 | 0.233 | 0.237 | 0.397 |
| c | -6.328 | -3.802 | -2.245 | -2.730 | -2.655 | -2.802 |
| Variance(c)(x10) | 0.360 | 0.220 | 0.189 | 0.199 | 0.202 | 0.336 |
| d | -1.362 | -1.192 | -0.502 | -0.131 | -0.061 | -0.720 |
| Variance(d)(x100) | 0.157 | 0.115 | 0.098 | 0.103 | 0.105 | 0.147 |
| e | -1.699 | -0.415 | 1.198 | 3.021 | 4.234 | 2.854 |
| Variance(e)(x10) | 0.432 | 0.310 | 0.266 | 0.280 | 0.284 | 0.403 |
| f | 1.980 | 0.090 | -2.838 | -5.456 | -6.585 | -3.881 |
| Variance(f)(x100) | 0.759 | 0.546 | 0.469 | 0.493 | 0.500 | 0.710 |
| g | 8.378 | 4.555 | 7.321 | 10.245 | 9.723 | 0.604 |
| Variance(g)(x10) | 1.609 | 1.173 | 1.008 | 1.059 | 1.075 | 1.504 |
| μ (x100) | 0.400 | -0.999 | -0.710 | -1.200 | -1.800 | 0.400 |
| σ (x10) | 6.204 | 5.251 | 4.963 | 4.800 | 6.126 | 6.049 |
| M_{\max} | 6.915 | 7.278 | 7.797 | 7.954 | 8.091 | 7.512 |
| h_{\max} | 4.291 | 22.978 | 2.111 | 2.769 | 3.214 | 3.677 |
| No. of Data | 360 | 540 | 540 | 540 | 540 | 360 |

TABLE V
(Continued)

HORIZONTAL COMPONENT

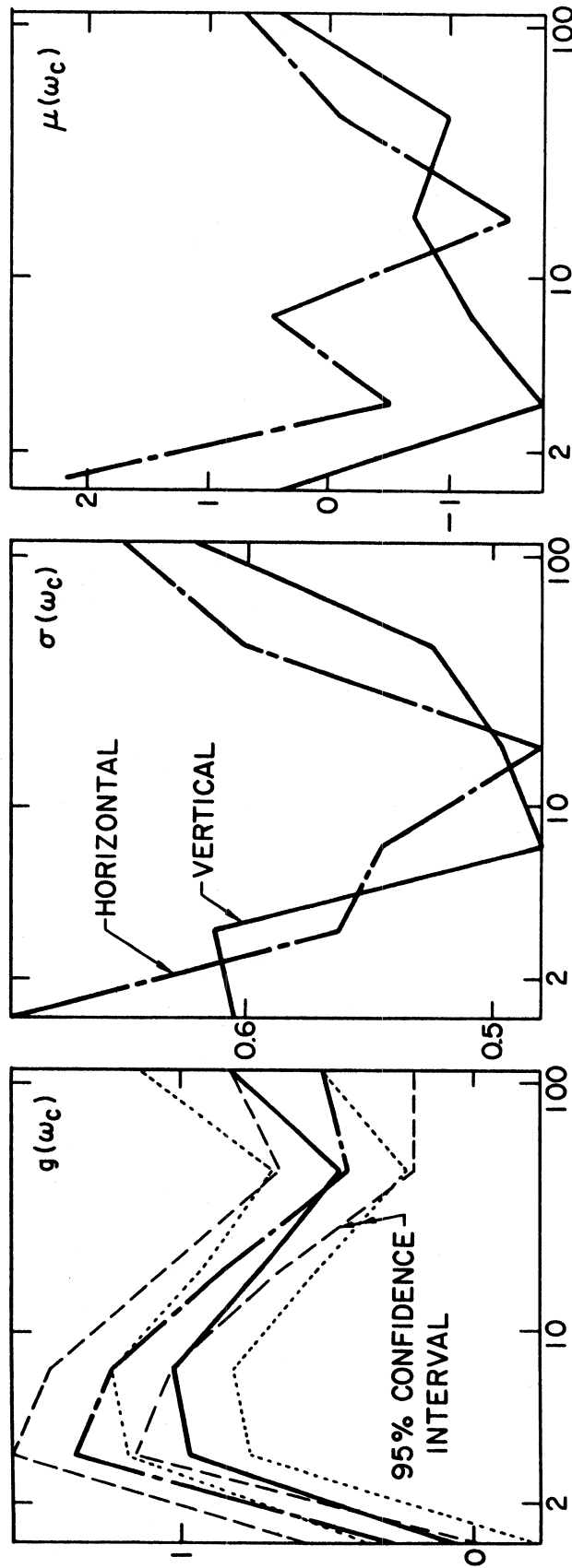
| | $f_c = 18$ | $f_c = 7$ | $f_c = 2.75$ | $f_c = 1.1$ | $f_c = 0.5$ | $f_c = 0.22$ |
|-------------------|------------|-----------|--------------|-------------|-------------|--------------|
| a | -2.055 | -1.103 | -0.517 | -0.483 | -0.647 | -1.197 |
| Variance(a)(x0.1) | 0.125 | 0.074 | 0.064 | 0.067 | 0.068 | 0.117 |
| b | 6.726 | 3.970 | 2.373 | 1.954 | 2.096 | 3.250 |
| Variance(b) | 0.425 | 0.258 | 0.222 | 0.233 | 0.237 | 0.397 |
| c | -4.733 | -2.509 | -1.269 | -0.747 | -0.756 | -1.869 |
| Variance(c)(x10) | 0.360 | 0.220 | 0.189 | 0.199 | 0.202 | 0.336 |
| d | -1.599 | -1.302 | -0.564 | 0.022 | 0.330 | -0.659 |
| Variance(d)(x100) | 0.157 | 0.115 | 0.098 | 0.103 | 0.105 | 0.147 |
| e | 0.139 | 0.405 | 1.342 | 3.342 | 5.319 | 6.584 |
| Variance(e)(x10) | 0.432 | 0.310 | 0.266 | 0.280 | 0.284 | 0.403 |
| f | -1.323 | -1.323 | -2.317 | -4.958 | -7.062 | -9.185 |
| Variance(f)(x100) | 0.759 | 0.546 | 0.469 | 0.493 | 0.500 | 0.710 |
| g | 5.174 | 4.304 | 8.588 | 12.381 | 13.621 | 2.640 |
| Variance(g)(x10) | 1.609 | 1.173 | 1.008 | 1.059 | 1.075 | 1.504 |
| μ (x100) | 0.700 | -0.100 | -1.520 | 0.460 | -0.530 | 2.600 |
| σ (x10) | 6.499 | 6.008 | 4.807 | 5.444 | 5.614 | 6.941 |
| M_{\max} | 7.106 | 7.913 | 9.352 | 13.071 | 13.859 | 8.695 |
| h_{\max} | 0.527 | 1.530 | 2.896 | 3.370 | 3.766 | 3.584 |
| No. of Data | 720 | 1080 | 1080 | 1080 | 1080 | 720 |



Center Frequency ω_c , rad/sec

FIGURE 11a

The coefficients a, b, c, d, e, and f in equation (20) for horizontal and vertical components of ground motion plotted versus $\omega_c = 2\pi f_c$ ($f_c = 0.22, 0.5, 1.1, 2.75, 7.0$ and 18.0 Hz). The coefficients are bounded by the calculated 95% confidence intervals.



Center Frequency ω_c , rad/sec

FIGURE 11b

The coefficients g , μ , and σ in equations (13) and (18) for horizontal and vertical components of ground motion plotted versus $\omega_c = 2 f_c$ (for $f_c = 18.0, 7.0, 2.75, 1.1, 0.5$ and 0.22 Hz). $g(\omega_c)$ is bounded by the calculated 95% confidence interval.

A comparison of the magnitude dependent term, $b(\omega_c)M + c(\omega_c)M^2$, for $\int_0^T a^2 dt$, in Figure 9 and for the average rate of growth of acceleration in Figure 12 shows the rate dependence on magnitude to be larger for almost all of the frequency bands, yet both sets of curves peak at approximately the same magnitudes, M_{\max} . At $M = M_{\max}$ the value of $bM + cM^2$ for the rates is about 0.15 (on the logarithmic scale) greater than the similar function for the integral correlations for the vertical motion. It is apparently 0.10 greater for the horizontal component.

Figure 12 also presents the values of $eh + fh^2$ for the smoothed e and f coefficients. These terms have maxima between 2 to 4 km for the lowest frequency bands. As with the correlations of the integrals, the confidence intervals for both $e(\omega_c)$ and $f(\omega_c)$ include zero at the two highest frequency bands, $f_c = 18.0$ and 7.0 Hz.

Figures 13a and 13b show the compound dependence of the average rate on the magnitude, epicentral distance, and depth of sediments for the frequency smoothed coefficients from equation (20) and for $\epsilon = 0$. For the vertical component (Figure 13a), the rate is about 5 times greater for a depth of 3 km than for a zero depth (or hard rock site) at $f_c = 0.22$ Hz, while at the high frequencies ($f_c = 18.0$ Hz) the rate is about 2.5 times greater for a zero depth than for $h = 4.5$ km. The variation of the average rates with depth is greater at the lower frequencies, $f_c = 0.22, 0.5, 1.1$ and 2.75 Hz, for horizontal motion than for vertical motion.

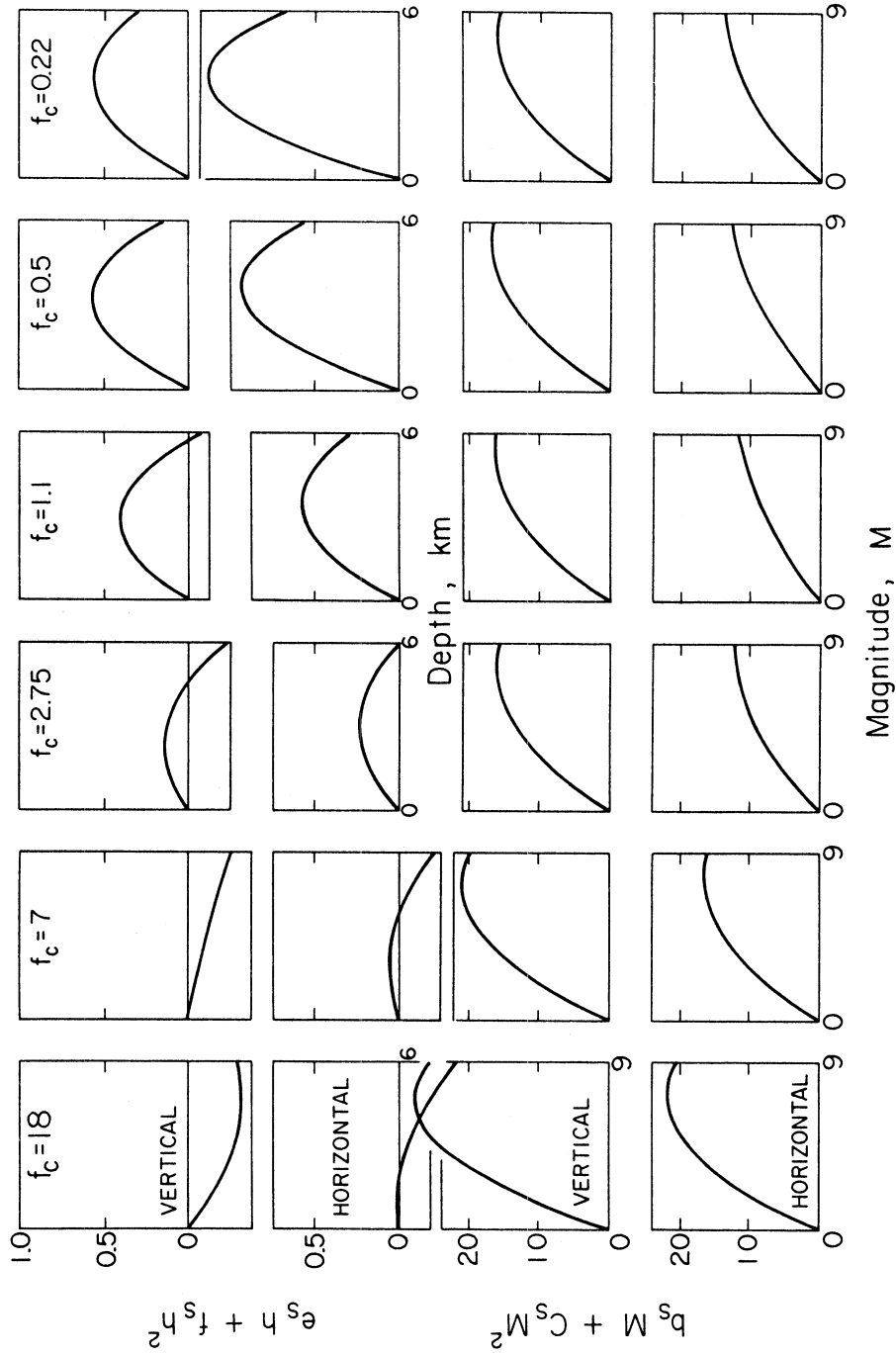


FIGURE 12

The values of $eh + fh^2$ (top) and $bM + cM^2$ (bottom) versus depth, h , and magnitude, M , respectively, using the frequency smoothed coefficients.

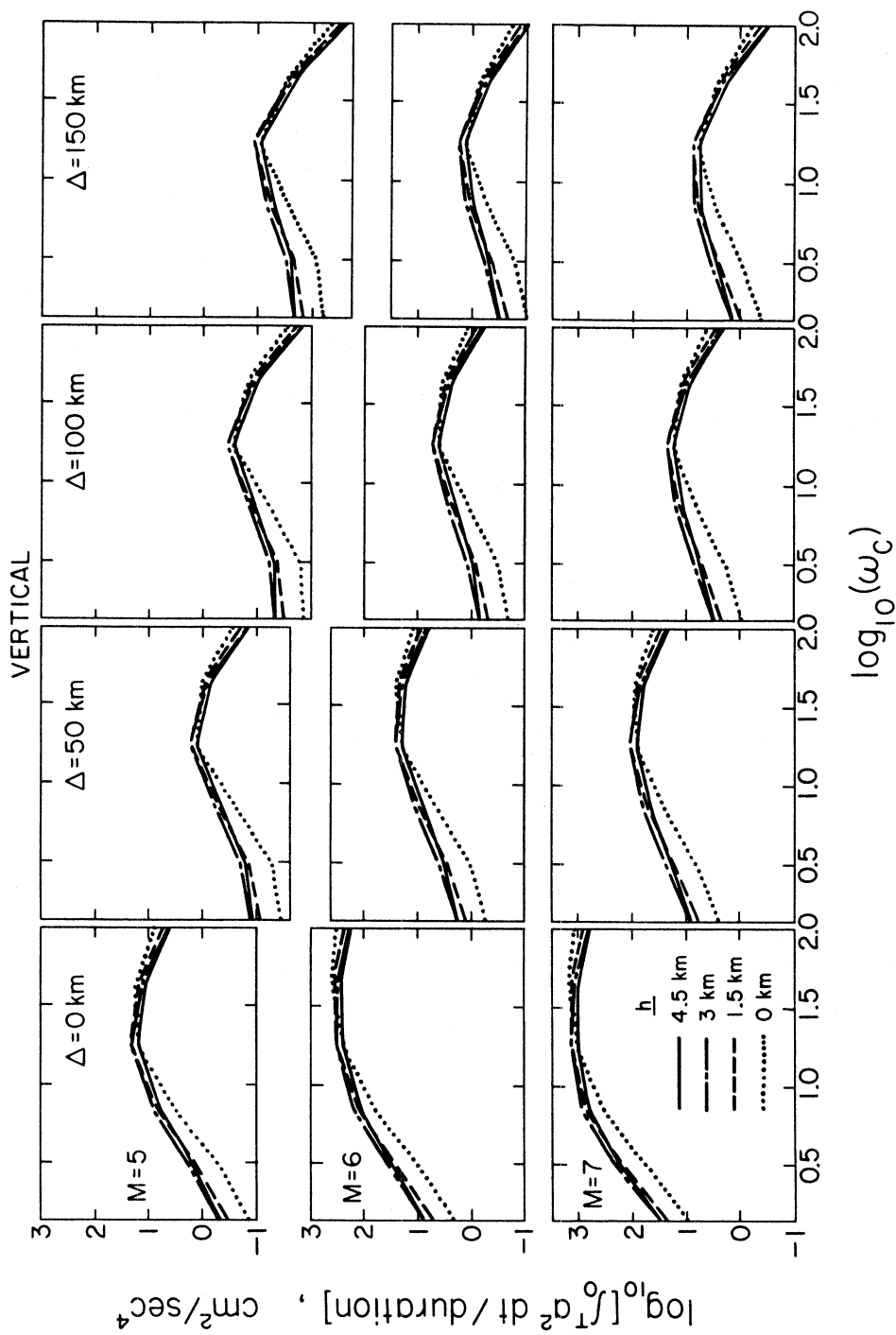


FIGURE 13a

The amplitudes of $\log_{10} \left[\int_0^T a^2(t) dt / \text{Duration} \right]$ computed from equation (20) (with $\epsilon = 0$, and using the frequency smoothed coefficients) for vertical motions versus frequency for selected magnitudes, epicentral distances and depth of sediments.

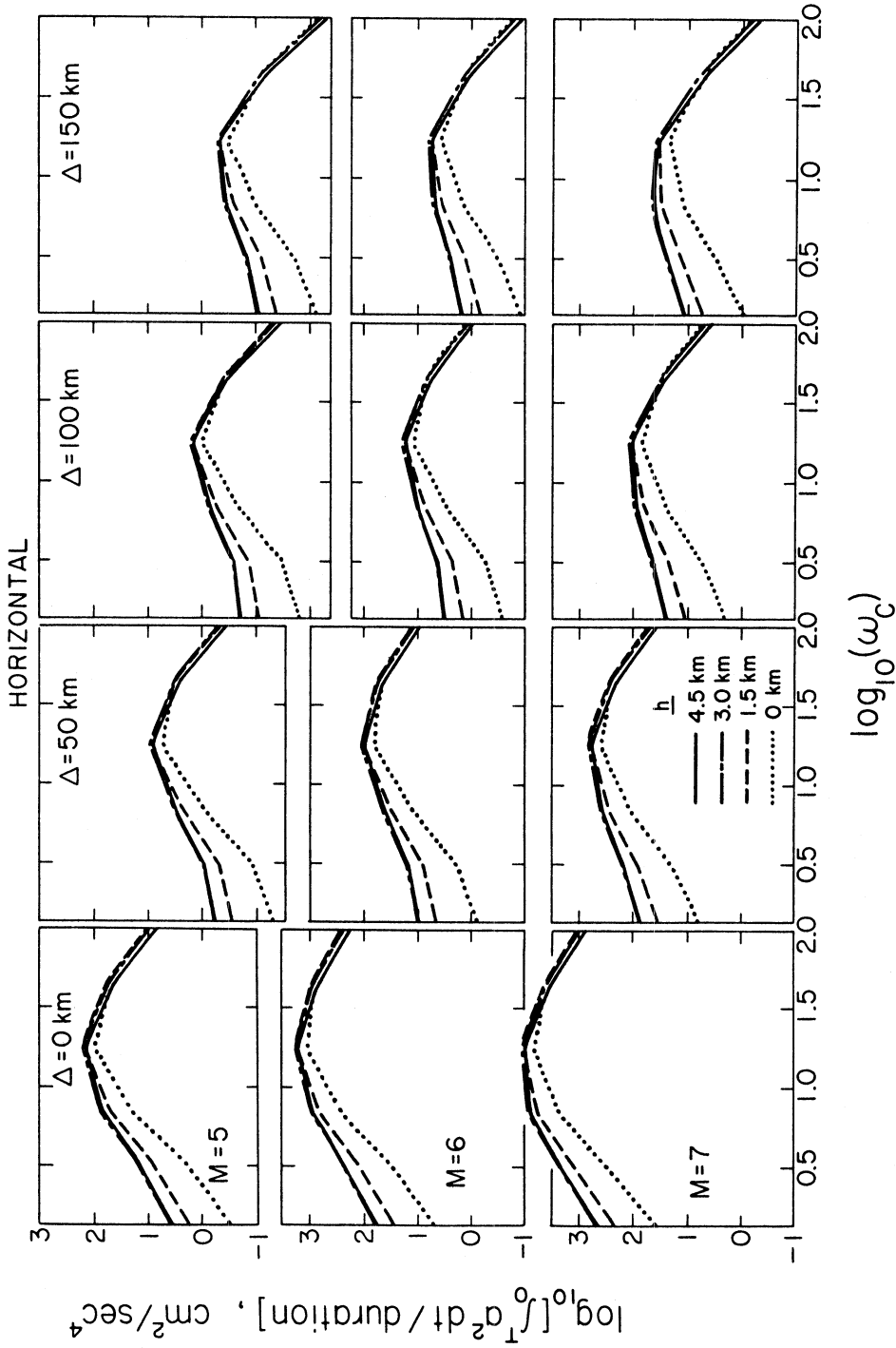


FIGURE 13b
 The amplitudes of $\log_{10} \left[\int_0^T a^2(t) dt / \text{Duration} \right]$ computed from equation (20) (with $\epsilon = 0$ and for the frequency smoothed coefficients) for horizontal motions versus frequency for selected magnitudes, epicentral distances, and depth of sediments.

CONCLUSIONS

In this report we have examined the effects of the depth of the sedimentary layer at the recording site on the duration, the integrals of the acceleration, velocity, and displacement squared, and the average rate of growth of these integrals through linear correlations. The simple model equations used in the regression analyses were identical to those used in our previous study (Trifunac and Westermo, 1976a) except that the recording site effects were parameterized in terms of the depth of sediments there instead of the simpler site classification, *s*.

For the regression analyses of the duration it was noted that the duration increased by as much as 2.1 sec/km of sediments at the two low frequency bands, $f_c = 0.5$ and 1.1 Hz, for the vertical component. At the two high frequency bands, $f_c = 18.0$ and 7.0 Hz, the duration increases by less than 0.5 sec/km. From the regression analysis with respect to the epicentral distance, it is seen that the duration increases by roughly 0.09 sec/km for $f_c = 0.2, 0.5, 1.1, 2.75$ and 7.0 Hz while at $f_c = 18.0$ Hz, it increases by about 0.14 sec/km.

From the dependence of $\log_{10} \int_0^T a^2 dt$ with depth (Figures 8a and 8b) it is seen that the integrals increase the most with depth for the lowest frequency band, $f_c = 0.22$ Hz, and for the horizontal component. The value of $\int_0^T a^2 dt$ was found to be as much as 14 times greater (on the linear scale) for a depth of 4 km than for a zero depth (or hard rock site). The maxima of these integrals were found to be at a depth of about 3 to 4 km for the four lowest frequency bands, $f_c = 2.75, 1.1, 0.5$ and 0.22 Hz.

The variation of the average rate with the depth of sediments is greater for the horizontal component than for the vertical, and for the low frequencies than the high. At the lowest frequency considered ($f_c = 0.22$ Hz), the rate is approximately 10 times greater for $h = 4.5$ km than for $h = 0$ for the horizontal component, and about 4 times greater for the vertical component.

ACKNOWLEDGEMENTS

We thank J.G. Anderson for critical reading of this manuscript and for useful suggestions.

This research was supported by a contract from the U.S. Nuclear Regulatory Commission.

Department of Civil Engineering
University of Southern California
Los Angeles, California 90007

References

- Anderson, J.G., and M.D. Trifunac (1977). On Uniform Risk Functionals which Describe Strong Earthquake Ground Motion: Definition, Numerical Estimation, and an Application to the Fourier Amplitude of Acceleration, Dept. of Civil Eng., Report No. 77-02, Univ. of Southern California, Los Angeles.
- Bolt, B.A. (1973). Duration of Strong Ground Motion, Proc. Fifth World Conf. on Earthquake Engineering, Rome, 6-D, Paper No. 292.
- Cartwright, D.E., and M.S. Longuet-Higgins (1956). The Statistical Distribution of the Maxima of a Random Function, Proc. Roy. Soc. London, Ser. A, 237, 212-232.
- Gutenberg, B., and C.F. Richter (1942). Earthquake Magnitude, Intensity, Energy and Acceleration, Bull. Seism. Soc. Amer., 32, 163-191.
- Gutenberg, B., and C.F. Richter (1956). Earthquake Magnitude, Intensity, Energy and Acceleration, Paper II, Bull. Seism. Soc. Amer., 46, 105-195.
- Hoel, P.G. (1971). Introduction to Mathematical Statistics, Fourth Edition, John Wiley and Sons, Inc., New York, 409p.
- Meyer, S.L. (1975). Data Analysis for Scientists and Engineers, John Wiley & Sons, New York.
- Richter, C.F. (1958). Elementary Seismology, Freeman & Co., San Francisco.
- Thatcher, W., and T.C. Hanks (1973). Source Parameters of Southern California Earthquakes, J. Geophys. Res., 78, 8547-8576.
- Trifunac, M.D., F.E. Udwadia, and A.G. Brady (1973). Analysis of Errors in Digitized Strong-Motion Accelerograms, Bull. Seism. Soc. Amer., 63, 157-187.
- Trifunac, M.D., and V.W. Lee (1973). Routine Computer Processing of Strong Motion Accelerograms, Earthquake Engr. Res. Lab., EERL Report No. 73-03, Calif. Inst. of Tech., Pasadena.
- Trifunac, M.D., and A.G. Brady (1975). A Study on the Duration of Strong Earthquake Ground Motion, Bull. Seism. Soc. Amer., 65, 581-526.
- Trifunac, M.D. (1976a). Preliminary Statistical Analysis of the Peaks of Strong Earthquake Ground Motion - Dependence of Peaks on

- Earthquake Magnitude, Epicentral Distance and Recording Site Conditions, submitted to Bull. Seism. Soc. Amer.
- Trifunac, M.D. (1976b). Preliminary Empirical Model for Scaling Fourier Amplitude Spectra of Ground Acceleration in Terms of Earthquake Magnitude, Source to Station Distance, and Recording Site Conditions, Bull. Seism. Soc. Amer., 67 (in press).
- Trifunac, M.D., and B.D. Westermo (1976a). Dependence of the Duration of Strong Earthquake Ground Motion on Magnitude, Epicentral Distance, Geologic Conditions at the Recording Site and Frequency of Motion, Dept. of Civil Eng., Report No. 76-02, Univ. of Southern California, Los Angeles.
- Trifunac, M.D., and B.D. Westermo (1976b). Correlations of Frequency-Dependent Duration of Strong Earthquake Ground Motion with the Modified Mercalli Intensity and the Geologic Conditions at the Recording Stations, Dept. of Civil Eng., Report No. 76-03, Univ. of Southern California, Los Angeles.
- Wong, H.L., and M.D. Trifunac (1977). A Note on the Effects of Recording Site Conditions on Amplitudes of Strong Earthquake Ground Motion, 2-119, Sixth World Conf. on Earthquake Eng., New Delhi, India.

APPENDIX I

The general linear regression problem can be summarized as follows: Given n observations of a function, y_i , along with m parameters for each observation, x_{ij} , we seek a set of m coefficients, c_j , such that

$$\begin{aligned} y_1 &= \sum_{j=1}^m x_{1j} c_j \\ y_2 &= \sum_{j=1}^m x_{2j} c_j \\ &\vdots \\ y_n &= \sum_{j=1}^m x_{nj} c_j \end{aligned} \tag{1}$$

or in a matrix form,

$$\underline{y} = X\underline{c} \tag{2}$$

with X being an $n \times m$ matrix. With $n \leq m$ a generalized inverse of X is found and \underline{c} can be written as

$$\hat{\underline{c}} = (X^T X)^{-1} X^T \underline{y} . \tag{3}$$

It can be shown that the coefficients, $\hat{\underline{c}}$, satisfy a least squares fit in equation (3) (Hoel, 1971).

To find the variances and covariances of these "best" coefficients the covariance of $\hat{\underline{c}}$ in equation (3) is taken yielding

$$\begin{aligned} [\text{cov}(\hat{\underline{c}})] &= \text{cov}[(X^T X)^{-1} X^T \underline{y}] \\ &= (X^T X)^{-1} X^T [\text{cov}(\underline{y})] [(X^T X)^{-1} X^T]^T . \end{aligned} \tag{4}$$

Assuming the independent y_i 's to have the same variance, σ^2 , equation (4) can be reduced to

$$[\text{cov}(\underline{\hat{c}})] = \sigma^2 (\underline{X}^T \underline{X})^{-1} . \quad (5)$$

The variance of the y's, σ^2 , is not known, however, so the unbiased estimate of the variance based on the computed coefficients $\underline{\hat{c}}$, $\hat{\sigma}^2$, is used, where

$$\hat{\sigma}^2 = \frac{1}{n-m} (\underline{y} - \underline{X}\underline{\hat{c}})^T (\underline{y} - \underline{X}\underline{\hat{c}}) . \quad (6)$$

The term $(\underline{y} - \underline{X}\underline{\hat{c}})^T (\underline{y} - \underline{X}\underline{\hat{c}})$ is the sum of the squared residuals of the model equation (2) applied to the n data points, and n-m is the number of degrees of freedom. The covariance matrix is given by

$$[\text{cov}(\underline{\hat{c}})] = \begin{bmatrix} \text{var}(\hat{c}_1) & \text{cov}(\hat{c}_1, \hat{c}_2) & \text{cov}(\hat{c}_1, \hat{c}_3) & \dots \\ \text{cov}(\hat{c}_2, \hat{c}_1) & \text{var}(\hat{c}_2) & \dots & \dots \\ \vdots & \vdots & \vdots & \vdots \\ \vdots & \vdots & \vdots & \vdots \end{bmatrix} \quad (7)$$

with the variance of each of the best fit coefficients, \hat{c}_i , being its respective diagonal element in this matrix.

The confidence interval for a coefficient, \hat{c}_j , based on an S% level of confidence is given by

$$\hat{c}_j \text{ accepted} = \hat{c}_j \pm t_{S\%, n-m} \sqrt{\text{var}(\hat{c}_j)} , \quad (8)$$

where t is the student T distribution function based on S% confidence and n-m degrees of freedom. For this study, a 95% level was chosen and thus $t_{95\%, n-m \leq 200} = 1.96$ was used in equation (8) for computing the significance bounds for the regression coefficient.